

**ANALYSIS OF SCATTERING EFFECT ON ZNO NANORODS
COATED GLASS SUBSTRATE TOWARDS HUMIDITY
DETECTION**

MUHAMMAD HAKIMI BIN ROSLAN

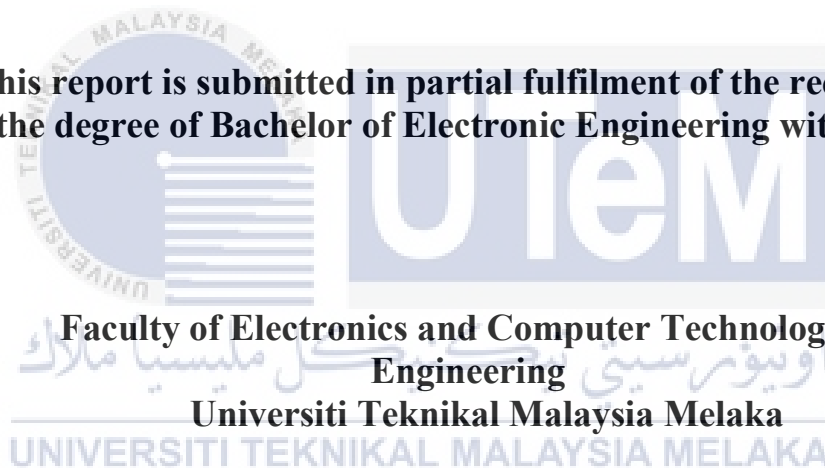


UNIVERSITI TEKNIKAL MALAYSIA MELAKA

**ANALYSIS OF SCATTERING EFFECT ON ZNO
NANORODS COATED GLASS SUBSTRATE TOWARDS
HUMIDITY**

MUHAMMAD HAKIMI BIN ROSLAN

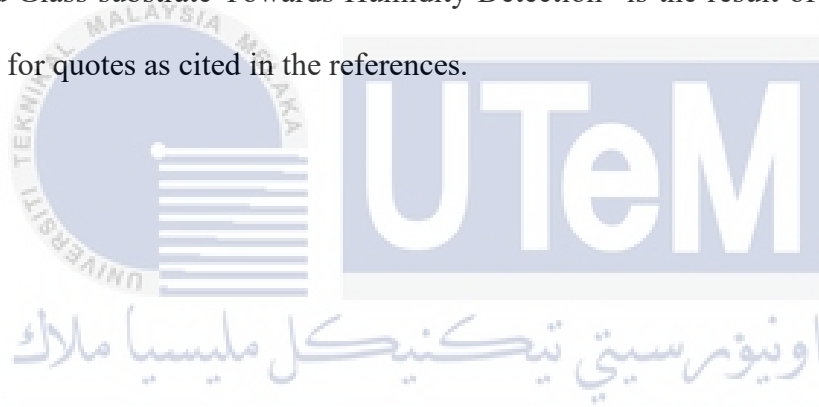
**This report is submitted in partial fulfilment of the requirements
for the degree of Bachelor of Electronic Engineering with Honours**



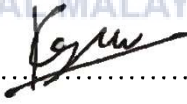
2024

DECLARATION

I declare that this report entitled “Analysis of Scattering Effect on ZnO Nanorods Coated Glass substrate Towards Humidity Detection” is the result of my own work except for quotes as cited in the references.



UNIVERSITI TEKNIKAL MALAYSIA MELAKA

Signature : 

Author : MUHAMMAD HAKIMI BIN ROSLAN

Date : 14 JUN 2024

APPROVAL

I hereby declare that I have read this thesis and in my opinion, this thesis is sufficient in terms of scope and quality for the award of Bachelor of Electronic Engineering with Honours



Signature :

Supervisor Name :

IR. DR. HAZIEZOL HELMI BIN MOHD YUSOF

Date :

16 JUNE 2024

UNIVERSITI TEKNIKAL MALAYSIA MELAKA

DEDICATION

Alhamdulillah prays to Allah because of favor and grace from Allah, this work is dedicated to Universiti Teknikal Malaysia Melaka (UTeM) who's without their requirement's this final year project wouldn't be possibly conducted. Besides that, this work is dedicated to my parents who have pass on love of giving and respect on the education that has demanded me to become a responsible and educated student. Never forget to my lecturer, I would like to thanks to my supervisor, Ir. Dr. Haziezol Helmi bin Mohd Yusof from Faculty of Electronics and Computer Technology and Engineering (FTKEK) who has given I courage, support, and guidance along my final year project. Also, thanks for giving me the knowledge and ideas on improvising this project. By all the above who has contributed support and courage to who's without this courage's dedicating it's over and over. I would doubtfully have a lot of confidence and wouldn't be brave enough to end this project perfectly and smoothly.

ABSTRACT

ZnO is one of sensitive materials utilized in optical sensors for humidity detection. However, previous researchers only presented their work either on forward or backward scattering in measuring modulation of light in response towards humidity sensing. This project presented valuable findings for researchers in selecting specific scattering direction towards better sensing performance in developing humidity sensing device. In this project, several glass substrates coated with ZnO nanorods for 3 h, 6 h and 9 h of growth durations via hydrothermal approach. The project utilized a 3D-printed sensor setup which consists of an LED and two photodiodes which served as light source and light detectors, correspondingly. The successfully fabricated glass substrate was placed in glass holder on 3D-printed sensing device that aligned between the LED and one of the photodiodes. The photodiode served as the measurement of backward scattering by the ZnO nanorods. Another photodiode was placed as close as possible at the tip of the ZnO nanorods which served as forward scattering measurement. The setup was placed in a controlled chamber which humidity was increased from 30% to 90% of RH levels and the measurements were done on all samples with different growth durations. It was found that the ZnO characteristics towards humidity levels was dominated by backward scattering across all samples of 3 h, 6 h and 9 h of growth times. The maximum reduction of 240

mV was observed on the backward scattering by sample with growth time of 9 h with sensitivity of 3.3 mV/% for the measurement of relative humidity from 30% to 90%.



ABSTRAK

ZnO adalah salah satu bahan sensitif yang digunakan dalam sensor optik untuk pengesanan kelembapan. Walau bagaimanapun, penyelidik terdahulu hanya membentangkan kerja mereka sama ada pada penyebaran ke hadapan atau ke belakang dalam mengukur modulasi cahaya sebagai tindak balas terhadap pengesanan kelembapan. Projek ini membentangkan penemuan berharga untuk penyelidik dalam memilih arah penyebaran tertentu ke arah prestasi pengesanan yang lebih baik dalam membangunkan peranti pengesan kelembapan. Dalam projek ini, beberapa substrat kaca disaluti dengan nanorod ZnO selama 3 jam, 6 jam dan 9 jam tempoh pertumbuhan melalui pendekatan hidroterma. Projek ini menggunakan persediaan sensor cetakan 3D yang terdiri daripada LED dan dua fotodiod yang berfungsi sebagai sumber cahaya dan pengesan cahaya. Substrat kaca yang berjaya difabrikasi diletakkan dalam pemegang kaca pada peranti pengesanan cetakan 3D yang diselaraskan antara LED dan salah satu fotodiod. Fotodiod berfungsi sebagai pengukuran penyebaran ke belakang oleh nanorod ZnO. Fotodiod lain diletakkan seberapa hampir yang mungkin di hujung nanorod ZnO yang berfungsi sebagai pengukuran penyebaran ke hadapan. Persediaan diletakkan dalam ruang terkawal di mana kelembapan dinaikkan dari 30% ke 90% tahap RH dan pengukuran dilakukan pada semua sampel dengan tempoh pertumbuhan yang berbeza.

Didapati bahawa ciri-ciri ZnO terhadap tahap kelembapan didominasi oleh penyebaran ke belakang merentas semua sampel dengan tempoh pertumbuhan 3 jam, 6 jam dan 9 jam. Pengurangan maksimum 240 mV diperhatikan pada penyebaran ke belakang oleh sampel dengan tempoh pertumbuhan 9 jam dengan kepekaan 3.3 mV/% untuk pengukuran kelembapan relatif dari 30% hingga 90%.



ACKNOWLEDGEMENTS

In the name of Allah, the Most Gracious and the Most Merciful, all praise is due to Allah for the strength and blessings bestowed upon me to complete this thesis. I extend my heartfelt appreciation to my supervisor, Ir. Dr. Haziezol Helmi bin Mohd Yusof, for his guidance and unwavering support. His constructive feedback and insightful suggestions have been instrumental in the success of this final year project.

I am grateful to my colleagues, particularly the Photonics Engineering Research Group, Muzammil, Ilyana, Aizat and Encik Fendi for their assistance and instruction in utilizing laboratory equipment and materials for this project. My gratitude also extends to my friends Zaffir, Salahuddin, Norman, and others for their companionship and moral support. I owe a debt of gratitude to my family, especially my parents, whose prayers and encouragement have been a constant source of motivation. Their support has been pivotal in the completion of this thesis. Lastly, I acknowledge my own perseverance and dedication to this endeavor. The commitment to work tirelessly without respite and to continually strive for excellence has been a personal journey of growth. I thank myself for maintaining authenticity and generosity throughout this process.

TABLE OF CONTENTS

Declaration	
Approval	
Dedication	
Abstract	i
Abstrak	iii
Acknowledgements	v
Table of Contents	vi
List of Figures	ix
List of Tables	xii
List of Symbols and Abbreviations	xiii
CHAPTER 1 INTRODUCTION	Error! Bookmark not defined.5
1.1 Background Project	Error! Bookmark not defined.6
1.2 Problem Statement	18
1.3 Objective	18
1.4 Scope of Project	19
1.5 Chapter Outlines	20

CHAPTER 2 LITERATURE REVIEW	21
2.1 Introduction	21
2.2 Optical Sensor	23
2.3 Types of Optical Sensor	25
2.4 Optical Sensor as Humidity Devices	24
2.5 Light Scattering	25
2.6 Light Scattering in Humidity Detection Application	27
2.7 Zinc Oxide as Sensing Element	29
2.8 Hydrothermal Fabrication of Zinc Oxide Nanostructures	30
2.9 Zinc Oxide Nanoparticles	31
2.10 Adsorption and Desorption processes of Water Molecules on ZnO Nanorods	31
2.11 Glass Substrate in Sensing Application	321
2.12 Arduino as Data Acquisition for Sensing Device	34
2.13 Op-Amp for Signal Conditioning	35
CHAPTER 3 METHODOLOGY	38
3.1 Introduction	38
3.2 Project Flowchart	39
3.3 Design of Body Sensor Setup	41
3.4 Circuit Implementation of Receiver	42
3.5 Materials and Equipment	44

3.6	Preparation of Glass Substrates	49
3.7	Preparation of Hydrothermal Process	51
3.7.1	Seeding Process	52
3.7.2	Growth Process	55
3.8	Humidity Sensing Experiment	55
3.9	Stability and Repeatability measurement	56
CHAPTER 4 RESULTS AND DISCUSSION		58
4.1	Fabricated Sensor Body Setup via 3D Printing	58
4.2	ZnO Nanorods on Glass substrates	59
4.3	Humidity Sensing Setup Integrate with Receiver circuit to Arduino Board	60
4.4	Linearity of Intensity	61
4.5	Humidity Response	62
4.6	Comparison ZnO Characteristics for Different Growth Time	66
4.7	ZnO Characterization for Different Growth Time	70
4.8	Stability Test Analysis	72
4.9	Environment and Sustainability	74
CHAPTER 5 CONCLUSION AND FUTURE WORKS		75
5.1	Conclusion	75
5.2	Future Work	76
REFERENCES		78

LIST OF FIGURES

Figure 2.1: Classification of humidity sensors by techniques and design	22
Figure 2.2: Types of Optical Sensors (a) Through-Beam Sensors, (b) Retro-Reflective Sensors, (c) Diffuse Reflection Sensors	24
Figure 2.3: Types of optical sensors. (a) Intrinsic (b) Extrinsic	25
Figure 2.4: Classification of Light Scattering	26
Figure 2.5: Rayleigh scattering and Mie scattering	27
Figure 2.6: Comparison between Rayleigh scattering and Raman scattering	27
Figure 2.7: Light scattered by a water droplet	28
Figure 2.8: Various nanostructures of zinc oxide (a) nanowires (b) nanorods (c) nanotubes (d) nanoflowers	29
Figure 2.9: The schematic of sensor fabrication process on glass substrates	33
Figure 2.10: Arduino UNO R3 layout.	34
Figure 2.11: Output display from the serial monitor in Arduino IDE	35
Figure 2.12: Diagram of an op-amp with terminals label	36
Figure 3.1: Project Flowchart	40
Figure 3.2: Dimension for (a) sensor body setup & Photodiode 1 holder (b) LED holder (c) Photodiode 2 holder	41
Figure 3.2.1: (a) Photodiode holder (b) LED holder (c) Glass substrate holder	42
Figure 3.3: A photodiode connected with Transimpedance Amplifier (TIA)	43
Figure 3.4: Glass substrate preparation process.	50

Figure 3.5: Measurement of glass substrates.	51
Figure 3.6: Flow of the Hydrothermal Process.	51
Figure 3.7: Flow of the Seeding Process.	52
Figure 3.8: Preparation of seeding solution	53
Figure 3.9: Masked samples seeding procedure.	53
Figure 3.10: Process of Seeding	54
Figure 3.11: Process of Annealing	54
Figure 3.12: Process of Growth	55
Figure 3.13: Schematic representation of the experimental setup for humidity sensor.	56
Figure 4.1: The 3D body sensor setup	59
Figure 4.2: ZnO nanorods coating in rectangular shapes on glass substrates for growth duration (a) 3 h (b) 6 h and 9 h.	59
Figure 4.3: Orthogonal overview for the (a) angle view, (b) top view, and (c) full sensor body setup for actual of humidity experiment conducted with integrated sensor device.	61
Figure 4.4: Forward Scattering Optical Characterization Towards Humidity Response with 3 h Growth Time samples	Error! Bookmark not defined. 3

No table of figures entries found.Figure 4.6: Forward Scattering Optical Characterization Towards Humidity Response with 6 h Growth Time samples**Error! Bookmark not defined.**4

No table of figures entries found.Figure 4.8: Forward Scattering Optical Characterization Towards Humidity Response with 9 h Growth Time samples**Error! Bookmark not defined.**5

No table of figures entries found.Figure 4.10: Forward Scattering Optical Characterization Towards Humidity Response with different Growth Time 67

Figure 4.11: Backward Scattering Optical Characterization Towards Humidity Response with different Growth Time **Error! Bookmark not defined.**9

Figure 4.12: Schematic representation of the sensor showing the substrates coated with ZnO nanorods 71

Figure 4.13: The forward sensor stability analysis 73

Figure 4.14: The backward sensor stability analysis 73



LIST OF TABLES

Table 3.1: List of Component.	Error! Bookmark not defined.	3
Table 3.2: Material used.	Error! Bookmark not defined.	3
Table 3.3: Equipment and Device used.	Error! Bookmark not defined.	5
Figure 4.1: Both Forward and Backward Scattering Optical Characterization Towards Humidity Response with 9 h Growth Time samples		63
Figure 4.2: Both Forward and Backward Scattering Optical Characterization Towards Humidity Response with 9 h Growth Time samples		65
Figure 4.3: Both Forward and Backward Scattering Optical Characterization Towards Humidity Response with 9 h Growth Time samples		66
Table 4.4: The output average voltage (ΔV) of forward scattering with different growth time 3 h, 6 h, and 9 h		65
Table 4.5: The output average voltage (ΔV) of backward scattering with different growth time 3 h, 6 h, and 9 h		66
Table 4.: The comparison of output average voltage (ΔV) for forward and backward scattering with different growth time 3 h, 6 h, and 9 h		68

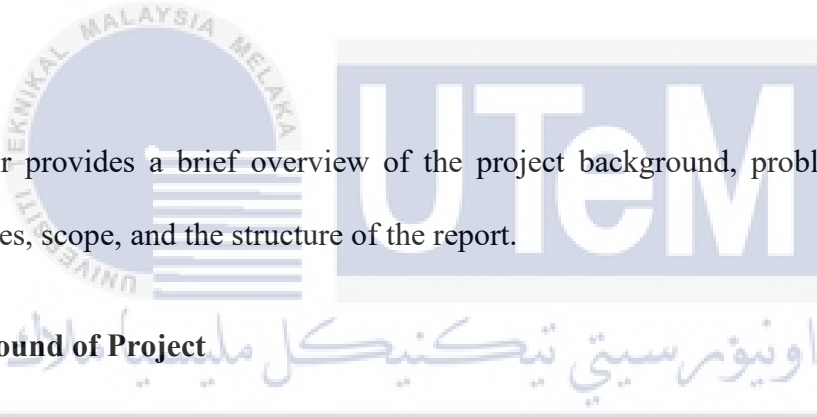
LIST OF SYMBOLS AND ABBREVIATIONS

ZnO	: Zinc Oxide
SnO ₂	: Tin Dioxide
WO ₃	: Tungsten Trioxide
TiO ₂	: Titanium Dioxide
LED	: light-emitting diode
IM/DD	: intensity-modulated/direct-detection
3D	: 3-Dimensional
PLA	: Polylactic Acid
GPS	: Global Positioning System
FOS	: Fiber Optical Sensing
RH	: Relative Humidity
AH	: Absolute Humidity
APDs	: Avalanche Photodiodes
P	: Positive
N	: Negative
AM	: Amplitude Modulation
FM	: Frequency Modulation
UV	: Ultraviolet
c	: Speed of light

ν	: Frequency
λ	: Wavelength
σ	: Sigma
n	: Refractive Index
I	: Intensity
CAD	: Computer Aided Design
TIA	: Transimpedance Amplifier
R_f	: Feedback Resistor
C_f	: Feedback Capacitor
Op - Amp	: Operational Amplifier
PCB	: Printed Circuit Board
$(CH_3)_2CO$: Acetone
CH_3CH_2OH	: Ethanol
NaOH	: Sodium Hydroxide
$Zn(CH_3COO)_2 \cdot (H_2O)_2$: Zinc Acetate Dihydrate
$C_6H_{12}N_4$: Hexamethylenetetramine (HMT)
$Zn(NO_3)_2 \cdot 6H_2O$: Zinc Nitrate Hexahydrate
DI Water	: Deionized water
PTFE	: Polytetrafluoroethylene
L	: Length
W	: Width
C	: Celsius
S1	: Sample 1
S2	: Sample 2
S3	: Sample 3

CHAPTER 1

INTRODUCTION



This chapter provides a brief overview of the project background, problem statement, project objectives, scope, and the structure of the report.

1.1 Background of Project

Humidity refers to the amount of water vapor or moisture present in the air or a gas. It is often expressed as a percentage and is a key factor in weather and climate. High humidity means that the air contains a significant amount of water vapor, while low humidity indicates that the air is relatively dry. Humidity levels can have various effects on human comfort, health, and the environment [1].

There are several methods to measure humidity levels, and one of the most effective solutions is using sensors. Today, sensors have become an integral part of our daily lives, with applications such as detecting force, pressure, flow, temperature, light, smoke, gas, alcohol, and more [2]. With the increasing development of industrialization, humidity sensors are being replaced by more effective solutions, with optical sensors emerging as a viable alternative.

Optical sensors have gained popularity due to their advantages, which include miniaturization, high sensitivity, fast response, and immunity to electromagnetic interference [3]. Optical sensors can employ various methods to measure humidity, and one of these methods involves the utilization of nanomaterials. The diverse range of nanomaterials, each possessing unique morphologies, chemical compositions, and specific surface properties, as well as distinctive crystalline structures, has led to their widespread adoption in chemical and optical sensing applications [4]. Among these nanomaterials, semiconducting metal oxides, such as Zinc oxide (ZnO), have significant consideration as a next age-band functional nanomaterial for sensing applications. Many researchers choose zinc oxide due to simplicity of fabrication, low price, optical properties, environmentally friendly and more [5].

In this work, ZnO nanorods were used as a sensing element for humidity detection due to the simplicity of fabrication and the good optical properties. The process of ZnO nanorods fabricating as sensing elements was take place on glass substrates by using low-temperature hydrothermal method because it did not require a high cost for that process. The sensing setup involves directing light from an LED that act as light source towards a photodiode, which serves as a photodetector. Based on the previous study, the investigation is to determine the efficiency of utilizing three color channels (red, green, and blue) towards the effect of the forward scattering for the vapors sensing performance. The results stated the green channel presented the highest relative intensity modulation (RIM) values, followed by the blue and red channels. Furthermore, this study has shown that the green channel is the best option for achieving better vapor sensing performance, especially towards the effects of forward scattering [8]. The setup were tested to analyze the scattering effect which to observe the dominant between forward and backward scattering towards humidity sensing.

1.2 Problem Statement

Forward and backward scattering are critical aspects in optical sensor technology, affecting the performance and capabilities of such sensors. The effect of forward and backward scattering in optical sensors has the ability to provide valuable data, enable selective detection, and support various applications across diverse industries, ranging from environmental monitoring and healthcare to research and development. Researchers in the past performed research on projects that used zinc oxide to detect humidity. The project's results have demonstrated a form of voltage levels that correspond with humidity [6]. Furthermore, they do not take consideration of the type of scattering effect on humidity detection. In this situation, the researchers are unsure if which direction of scattering is more dominant in producing higher sensing response for detecting humidity. Therefore, the goal of this project is to identify the type of scattering either forward or backward is more dominant when it comes to humidity detection. To analyze the scattering effect, a setup structure for forward and backward scattering measurement using glass substrate is required.

1.3 Objective

Based on the problem statements outlined in the previous section, the following objective is stated for this research:

1. To develop a sensing setup structure via 3D printer with built-in receiver circuit for forward and backward scattering measurement on the zinc oxide coated glass substrates.
2. To fabricate Zinc Oxide nanorods on the surface of glass substrates at growth duration of 3 h, 6 h and 9 h.
3. To analyze the forward and backward scattering by ZnO nanorods in the effect on humidity detection of scattering mechanism.

1.4 Scope of Project

The primary objective of this project is to analyze the dominant between forward and backward scattering in producing higher sensing response for detecting humidity. This were accomplished by designing a setup structure for forward and backward scattering measurement using coated glass substrates.

The first step in the analysis of scattering effect on ZnO nanorods coated glass substrate towards humidity detection is to develop a sensing setup structure by using Ender 3D Pro Printer for forward and backward scattering measurement on the fabricated glass substrate. This setup must require a pair of SFH203 photodiodes and a green LED with central wavelength 530nm to attached to it. These parts need to be firmly secured in place on the setup. The only thing that can be changed is the glass with a coating, and it can be replaced with another few coated glass with a different growth duration.

After that, the next step is to fabricate Zinc Oxide nanorods on the surface of several glass substrates at different growth durations. The ZnO nanorods were fabricated by using the hydrothermal method on several glass substrates with three growth durations (3 hours, 6 hours, and 9 hours).

Once the sensing setup structure and ZnO coated with the glass substrates are complete, the analysis undergoes in a controlled chamber. Analysis involves Arduino uno R3 as microcontroller, receiver circuit incorporates the LT1884 op-amp chip, pair of SFH203 photodiodes as light detector. The pair of SFH203 photodiodes were used to served as the measurement of backward scattering by the ZnO nanorods while the other photodiode served as forward scattering and were placed as closed as possible at the tip of the ZnO nanorods. The LCD display is to show a voltage output with a various coated glass substrate growth duration

through humidity detection. By comparing the performance recorded from a both scattering effect, it helps validate which are more dominant between forward scattering and backward scattering effect towards humidity detection.

1.5 Chapter Outlines

This thesis consists of five chapters demonstrating the Analysis of Scattering Effect on ZnO Nanorods Coated Glass Substrate Towards Humidity Detection.

Chapter 1 gave an introduction about the project as well as problem statement, objective and project scope of the project.

Chapter 2 reviews the related literature on the topics of sensors, glass substrate, optical sensors, nanomaterials, and ZnO particles.

Chapter 3 explains in detail the methodology briefly. This chapter discusses the implementation of hardware and software. It also includes a fabrication process of ZnO nanomaterials glass substrates. The optical optimization on the effect of growth conditions of the fabricated ZnO nanorods.

Chapter 4 presents project outcomes and the associated costs are presented based on the three objectives.

Chapter 5 presents the project accomplishments are presented based on the three objectives outlined in Chapter 1. The chapter also provides some ideas for future enhancements.

CHAPTER 2

LITERATURE REVIEW

In this chapter, all previous related projects that have a few similarities with the project are reviewed. By learning from what others have done, this project can be better and have more ideas. Some of the papers also give their suggestions for continuing their project, which can help this project as it tries to do something new that no one has done before.

2.1 Introduction

Sensors are devices that can sense and measure various physical, chemical, or biological properties of the environment. They are widely used in different industries for various purposes, such as monitoring and controlling systems and equipment. Sensors are also part of our everyday life, as they can detect various phenomena, such as force, pressure, flow, temperature, light, smoke, gas, alcohol, and more. Sensors can produce different types of electrical outputs, such as voltage, current, capacitance, resistance, frequency, or other signals that vary over time, depending on the sensor type [7].

When it comes to measuring humidity, various methods exist, with sensors standing out as a highly effective solution. There are several methods to measure humidity levels, and one of the most effective solutions is using sensors. Sensors in various industries are used for

different applications, both in routine and commercial. Sensors link multiple devices and enable various machines to communicate to track systems and equipment at each facility [8].

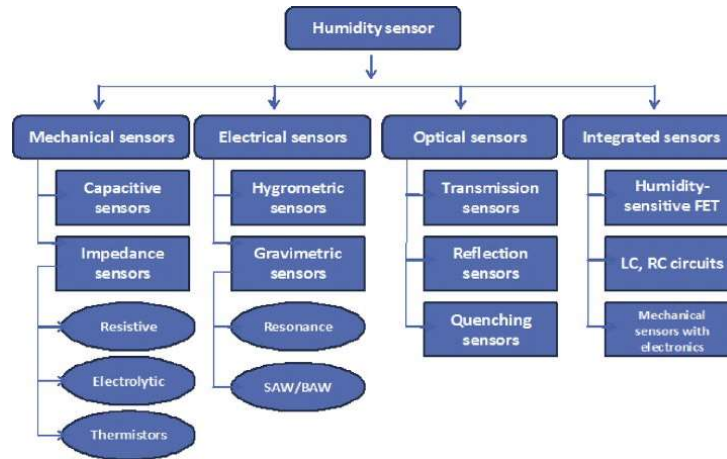


Figure 2.1: Classification of humidity sensors by techniques and design

Figure 2.1 shows the classification of humidity sensors by techniques and design. Electronic sensors measure physical changes in materials that can absorb water vapor, including substances like animal hair and paper coils [9]. However, these methods have often proven to be inaccurate, with limited measurement ranges and high maintenance demands. Additionally, electronic humidity sensors can degrade over time due to factors like dust, oil, and exposure to harmful gases, leading to reduced accuracy with extended use. In this context, electronic sensors may not be the most suitable choice for specific applications such as food processing, agriculture, medical settings, and pharmaceutical or laboratory environments [10]. Humidity sensors measure relative humidity, but they are being replaced by more effective solutions, such as optical sensors. The amount of vapour present in unit volume of air is called the absolute humidity of air. The formula for calculating relative humidity (RH) is [11]:

$$RH = \left(\frac{\text{Actual Vapor Pressure}}{\text{Saturation Vapor pressure at the Same Temperature}} \right) \times 100\% \quad (1)$$

Optical sensors use light to sense humidity, and they have many benefits, such as being small, sensitive, fast, and immune to electromagnetic interference.

2.2 Optical Sensor

Optical sensors are devices that use light to measure or detect various physical, chemical, or biological phenomena. They work by converting light rays into electrical signals that can be read by an integrated measuring device. Optical sensors have many advantages over other types of sensors, such as high sensitivity, accuracy, selectivity, speed, and immunity to electromagnetic interference. Optical sensors have various applications in different fields, such as communication, medicine, industry, agriculture, and environmental monitoring. Some examples of optical sensors are photodiodes, phototransistors, photomultipliers, CCDs, LEDs, lasers, fiber optics, and spectrometers [12].

The basic principle of optical sensors is to transmit and receive light in an optical sensor. The object to be detected reflects or blocks the light beam sent by an emitting diode. The deflection or reflection of the light beam is evaluated depending on the type of device. This makes it possible to find the object independently of the material it is made of, such as wood, metal, plastic, or other. The special device also allows for the detection of transparent objects or different colors or contrasting variations [13]. There are different types of optical sensors, such as through-beam, retro-reflective, and diffuse reflection as shown in Figure 2.2.

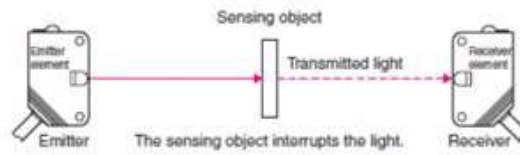
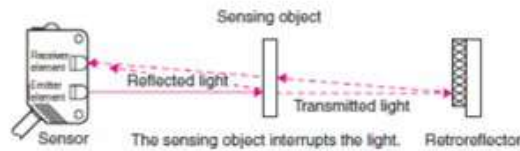
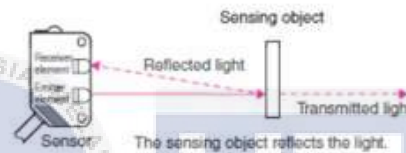
(a) Through-beam Sensors**(b) Retro-reflective Sensors****(c) Diffuse-reflective Sensors**

Figure 2.2: Types of Optical Sensors (a) Through-Beam Sensors, (b) Retro-Reflective Sensors, (c) Diffuse Reflection Sensors [14]

Through-beam sensors consist of two separate components, the transmitter and the receiver, that are placed opposite to each other. The transmitter projects a light beam onto the receiver. An interruption of the light beam is interpreted as a switch signal by the receiver. It is irrelevant where the interruption occurs. Retro-reflective sensors have the transmitter and receiver in the same house and use a reflector to direct the emitted light beam back to the receiver. An interruption of the light beam initiates a switching operation. Where the interruption occurs is of no importance. Diffuse reflection sensors also have the transmitter and receiver in the same house, but do not use a reflector. Instead, they rely on the object itself to reflect the light beam back to the receiver. The amount of light reflected depends on the distance, shape, and surface of the object [14].

2.3 Types of Optical Sensor

Optical sensors come in various types, primarily categorized as Extrinsic and Intrinsic as shown in Figure 2.2.1. Extrinsic optic sensors use the optical fiber as a carrier of light from a source to a detector.

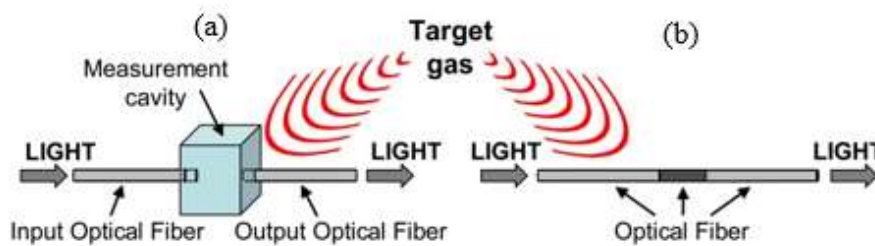


Figure 2.3: Types of optical sensors. (a) Intrinsic (b) Extrinsic [49]

The light signal is affected by an external transducer that changes its intensity, phase, polarization, wavelength, or direction. The detector then measures the change in the light signal and converts it into an electrical signal. Extrinsic sensors are usually less sensitive, less expensive, and easier to multiplex than intrinsic sensors [15]. While Intrinsic optical sensors use optical fiber as both the carrier and the modulator of light. The light signal is affected by the physical phenomenon directly inside the fiber, without leaving it. The change in the light signal can be detected by measuring the backscattered or reflected light from the fiber. Intrinsic sensors are usually more sensitive, more expensive, and more difficult to multiplex than extrinsic sensors [15].

2.4 Optical Sensor as Humidity Devices

Optical sensors can employ various methods to measure humidity. One of the methods that optical sensors can employ to measure humidity is the utilization of nanomaterials.

Nanomaterials are materials that have at least one dimension in the nanoscale range (1–100 nm). Nanomaterials have unique optical, electrical, mechanical, and chemical properties that depend on their size, shape, and composition. Nanomaterials can be used as sensing elements or coatings for optical sensors, enhancing their performance and functionality [16].

2.5 Light Scattering

Light scattering is a process that occurs when light waves encounter particles in a medium, such as air, water, or solid materials. The particles can reflect, refract, diffract, or absorb the light waves, changing their direction, wavelength, intensity, or polarization. The amount and characteristics of scattered light depend on several factors, such as the wavelength of the incident light, the size, shape, and refractive index of the particles, the angle of incidence, and the distance between the particles [17]. Light scattering can be classified into two types which are elastic and inelastic as shown in Figure 2.3.



Figure 2.4: Classification of Light Scattering [50]

Elastic scattering is when the scattered light has the same wavelength as the incident light, while inelastic scattering is when the scattered light has a different wavelength than the incident light [18].

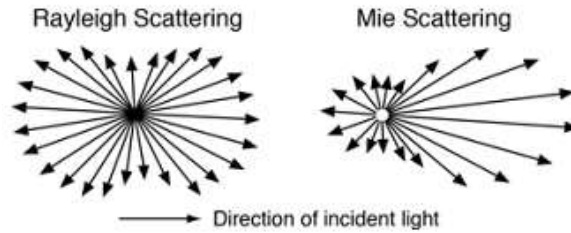


Figure 2.5: Rayleigh scattering and Mie scattering [51]

Figure 2.3.1 shows the examples of elastic scattering are Rayleigh scattering, which occurs when the particles are much smaller than the wavelength of the light, and Mie scattering, which occurs when the particles are comparable or larger than the wavelength of the light.

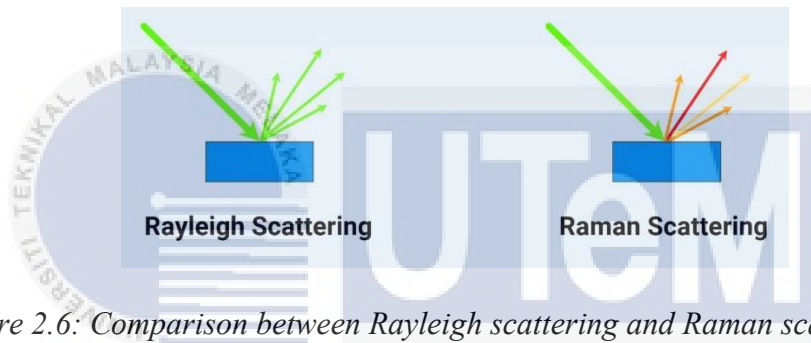


Figure 2.6: Comparison between Rayleigh scattering and Raman scattering [52]

Figure 2.3.2 shows the comparison between Rayleigh scattering and Raman scattering which occurs when the scattered light has a lower or higher frequency than the incident light due to the vibrational or rotational modes of the molecules, and Brillouin scattering, which occurs when the scattered light has a lower or higher frequency than the incident light due to the acoustic waves in the medium [19].

2.6 Light Scattering in Humidity Detection Application

Light scattering can be used for humidity detection applications, as the humidity level affects the size, shape, and refractive index of the particles in the air, which in turn affect the amount and intensity of scattered light [20]. Figure 2.4 shows the light scattered by a water droplet.

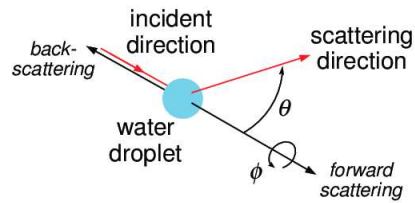


Figure 2.7: Light scattered by a water droplet [53]

Humidity is the amount of water vapor in the air, which can vary depending on the temperature, pressure, and location. Humidity can be measured in different ways, such as relative humidity, which is the ratio of the partial pressure of water vapor to the equilibrium vapor pressure at a given temperature, or absolute humidity, which is the mass of water vapor per unit volume of air. Humidity can affect the physical and chemical properties of the particles in the air, such as dust, smoke, pollen, or aerosols, which can absorb moisture and grow in size or change their shape when the humidity is high. [21] This can result in more light scattering, as the particles become more comparable or larger than the wavelength of the light and enter the Mie scattering regime. Moreover, humidity can also affect the refractive index of the particles, which is the ratio of the speed of light in a vacuum to the speed of light in the medium. The refractive index of the particles can change with humidity, as the water molecules can interact with the surface or the bulk of the particles, altering their optical properties. This can also result in more light scattering, as the refractive index contrast between the particles and the air increases [22].

2.7 Zinc Oxide as Sensing Element

Zinc oxide is a widely used material for sensing applications because of its unique properties, such as high sensitivity, selectivity, stability, and low cost. Compared to other metal oxides, such as tin oxide, titanium dioxide, indium oxide, and nickel oxide, zinc oxide has some advantages that make it a better choice for sensing element.

One of the main reasons why zinc oxide is preferred over other metal oxides is its ability to form various nanostructures, such as nanowires, nanorods, nanotubes and nanoflowers [23].

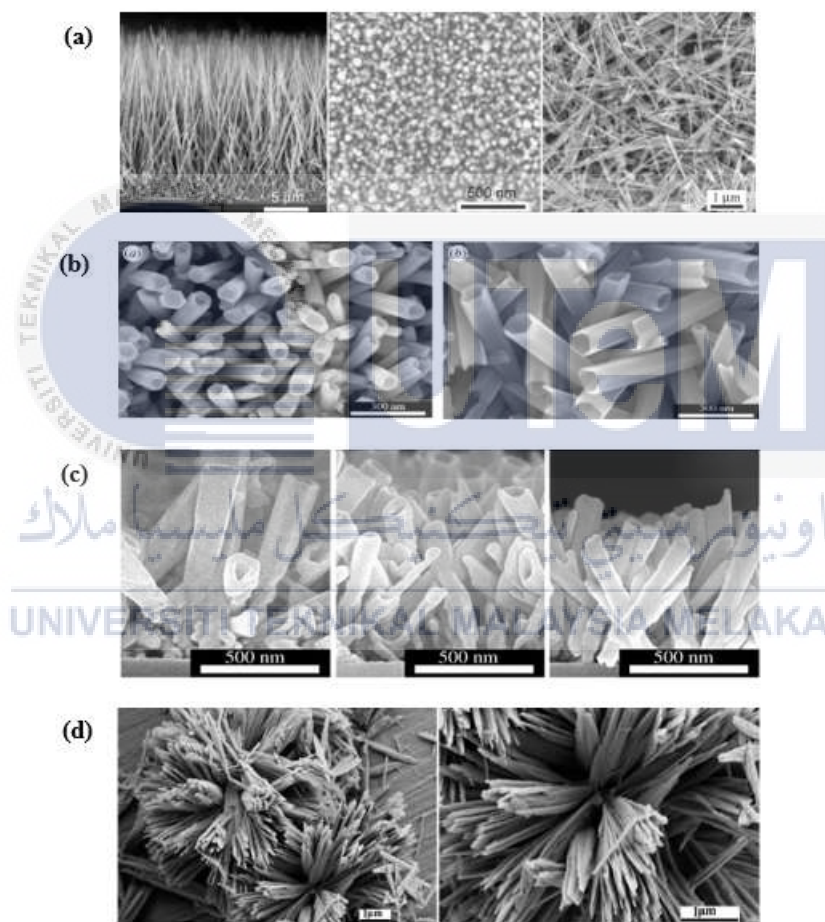


Figure 2.8: Various nanostructures of zinc oxide (a) nanowires (b) nanorods (c) nanotubes (d) nanoflowers [54]

Figure 2.5 shows the various nanostructures of zinc oxide. These nanostructures have a large surface area to volume ratio, which enhances the interaction between the gas molecules

and the sensing surface, resulting in higher sensitivity and faster response. Another reason why zinc oxide is superior to other metal oxides is its low operating temperature, which reduces the power consumption and prolongs the lifetime of the sensor. Zinc oxide can operate at room temperature or slightly above, while other metal oxides require higher temperatures (above 200°C) to activate their sensing mechanism. Zinc oxide also has a wider band gap (3.37 eV) than other metal oxides, which means it can absorb more UV light and generate more electron-hole pairs. This increases the conductivity of the sensor and improves its performance [24]. Furthermore, zinc oxide has a high chemical stability and resistance to corrosion, which makes it suitable for harsh environments. Zinc oxide is also biocompatible and eco-friendly, which are desirable features for biomedical and environmental applications. Zinc oxide is chosen over other metal oxides as sensing element because of its high sensitivity, selectivity, stability, low cost, and versatility in nanostructure fabrication. Zinc oxide can also operate at low temperatures, absorb more UV light, and resist corrosion, which are beneficial for sensing applications [25].

2.8 Hydrothermal Fabrication of Zinc Oxide Nanostructures

The choice of a fabrication method can significantly influence the structural characteristics and performance of the product. The hydrothermal process has employed over other fabrication process because it can create special crystalline phases that wouldn't be stable at normal melting points, leading to unique materials with unique properties [26]. Secondly, it is inexpensive since it avoids the use of high temperature and complex vacuum. Furthermore, it uses water as a solvent, which is easy to get, cheap, and environmentally friend [27].

2.9 Zinc Oxide Nanoparticles

A variety of semiconducting material oxides, including Zinc Oxide (ZnO), Titanium Dioxide (TiO₂), Tin Oxide (SnO₂), and Tungsten (VI) Oxide (WO₃), have been employed in the construction of gas sensors [28]. These materials act as gas-sensitive elements, with properties like conductance that alter when gas molecules are absorbed onto their surfaces. ZnO, in particular, is extensively utilized in gas sensing applications due to its excellent chemical stability, electrical compatibility, biocompatibility, and superior electron transfer properties [29]. As an n-type semiconductor, ZnO boasts a direct and wide band gap energy of 3.37 eV along with a significant exciton binding energy of 60mV [30]. Its straightforward, cost-effective, and eco-friendly fabrication process renders ZnO a favored material among researchers. Additionally, ZnO's high optical transparency within the visible spectrum renders it suitable for applications in short-wavelength optoelectronics, resonators, biosensors, and medical devices.

2.10 Adsorption and Desorption Processes of Water Molecules on ZnO Nanorods

The interaction of water molecules with ZnO nanorods is a complex process that significantly influences the performance of gas sensors. During adsorption, water molecules are attracted to and held on the surface of ZnO nanorods due to polar forces. The ZnO surface contains charged sites that can interact with the dipole moment of water molecules, leading to a physical or chemical bond. Physical adsorption involves weak van der Waals forces, while chemical adsorption involves the formation of stronger covalent or ionic bonds [31].

The adsorbed water molecules can alter the conductance of ZnO nanorods by either donating or accepting electrons, which changes the charge carrier concentration on the surface. This change in conductance is what allows ZnO nanorods to detect the presence of gases. When gas molecules displace the adsorbed water, there is a measurable change in electrical resistance.

Desorption is the counter process where adsorbed water molecules leave the ZnO surface. This can happen spontaneously at room temperature due to thermal energy, but it can be accelerated by increasing temperature. The desorption rate is crucial for sensor recovery time which is the time it takes for a sensor to return to baseline conductance after detecting a gas.

Both adsorption and desorption are influenced by environmental conditions. For instance, high humidity levels can increase the number of water molecules available for adsorption, potentially affecting sensor sensitivity. Conversely, high temperatures can promote desorption, clearing the sensor surface more quickly for subsequent gas detection events [32]. Understanding these processes is essential for optimizing ZnO nanorod-based sensors in terms of selectivity, sensitivity, response time, and recovery time.

2.11 Glass Substrate in Sensing Application

A glass substrate, a thin layer of glass, proves to be a versatile material for various sensing applications, including humidity, temperature, pressure, gas, and biosensors. Opting for a glass substrate offers several advantages compared to other materials. Firstly, its transparency allows light to pass through, facilitating interaction with the sensing elements. Additionally, its chemical inertness prevents corrosion and contamination, ensuring the integrity of the sensing elements [33].

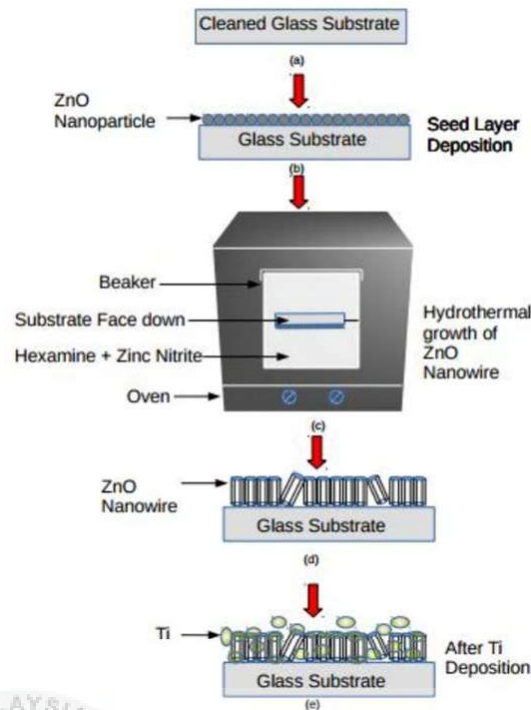


Figure 2.9: The schematic of sensor fabrication process on glass substrates [34]

The glass substrate's thermal stability reduces the impact of temperature fluctuations on sensor performance, while its mechanical robustness enhances durability. Moreover, the compatibility with diverse fabrication techniques, such as thin film deposition, etching, lithography, and bonding, enables the integration of different sensing elements and electronic components on the same substrate [35]. Examples of sensors utilizing glass substrates include scintillation detectors, thin film-based sensors, fiber optic sensors, and nanomaterial-based sensors. Despite its versatility and promise, there are challenges, such as choosing the right glass composition and fabrication process, ensuring proper sensor integration and packaging, and addressing calibration and validation issues for accurate and reliable measurements. Overall, the glass substrate stands as a promising material for sensors, offering high performance, cost-effectiveness, and the potential for sensor miniaturization [36].

2.12 Arduino as Data Acquisition Platform for Sensing Device

Arduino is a popular open-source platform for developing electronic projects, such as sensors, robots, and interactive art. Arduino can also be used as a data acquisition platform for sensing devices, which are instruments that measure physical quantities such as temperature, pressure, light, sound and more. Data acquisition is the process of collecting, processing, and storing data from sensors for analysis, visualization, or control purposes. One of the advantages of using Arduino as a data acquisition platform is that it is easy to use, inexpensive, and compatible with a wide range of sensors and modules. Arduino boards have analog and digital input/output pins that can interface with various sensors and actuators [37]. Arduino also has a built-in analog-to-digital converter (ADC) that can convert analog signals from sensors into digital values that can be read by the microcontroller. Arduino can communicate with a computer or other devices using serial, USB, Bluetooth, Wi-Fi, or other protocols, and send or receive data in various formats [38]. Figure 2.8 shows the Arduino UNO R3 layout.

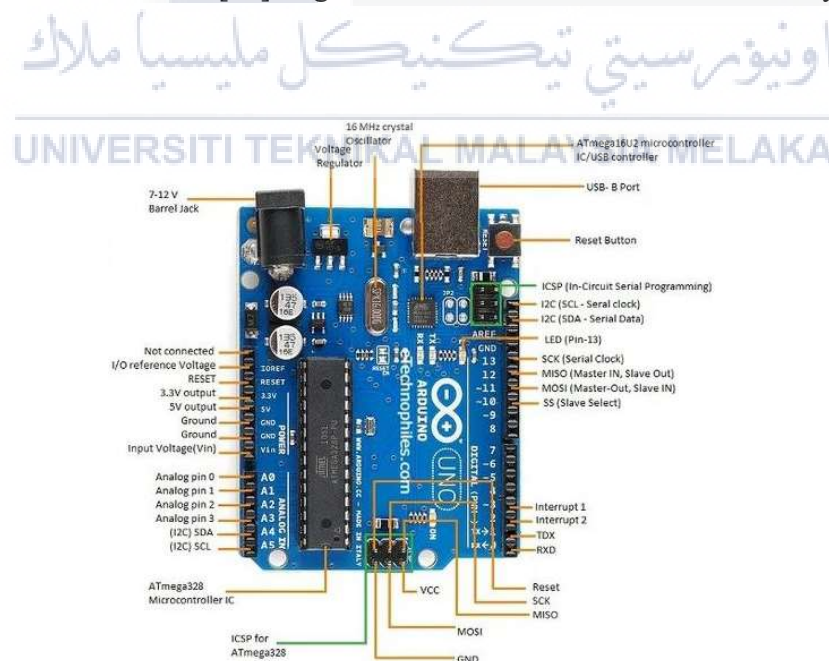


Figure 2.10: Arduino UNO R3 layout [38].

Another advantage of using Arduino as a data acquisition platform is that it can be programmed using the Arduino IDE, which is a user-friendly software that supports multiple programming languages, such as C, C++, and Python. The Arduino IDE provides a library of functions and examples that can simplify the coding process and help users to implement various functionalities, such as reading sensor data, performing calculations, displaying results, logging data and more further function. The Arduino IDE also allows users to upload their code to the Arduino board and monitor the serial output using a serial monitor or a serial plotter [39]. Figure 2.8.1 [39] shows the output display from the serial monitor in Arduino IDE.

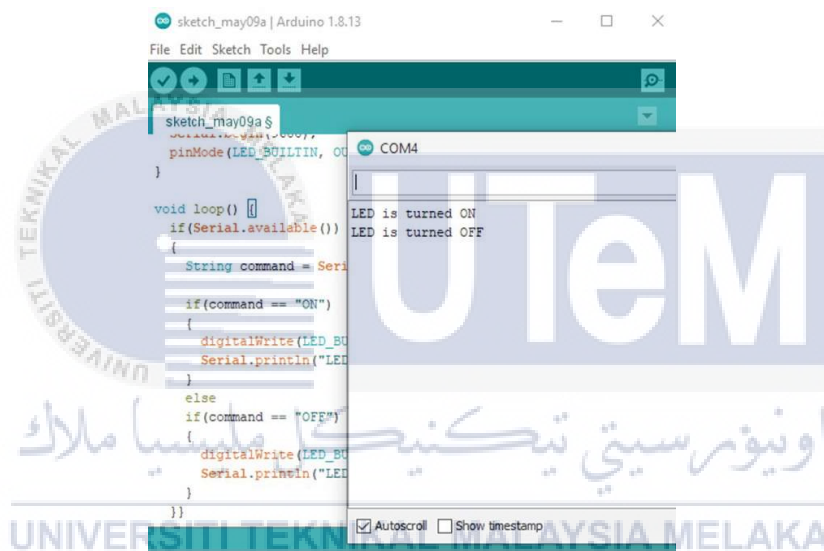


Figure 2.11: Output display from the serial monitor in Arduino IDE.

2.13 Op-Amp for Signal Conditioning

Op-amp signal conditioning involves adjusting the output signal of an operational amplifier (op-amp) to meet specific application needs. Op-amps are commonly used to amplify, filter, or perform mathematical operations on analog signals, like those from sensors. An operational amplifier, or op-amp, features five terminals: V_+ , V_- , $+V$, $-V$, and V_{out} , each

serving a specific function. Figure 2.9 shows the op-amp diagram of an op-amp with terminals label [40].

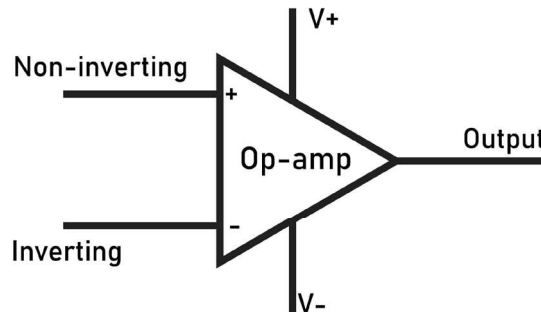


Figure 2.12: Diagram of an op-amp with terminals label.

$V+$ and $V-$ act as input terminals, commonly known as inverting and non-inverting terminals, respectively. The input signal is applied to one of these terminals, with the other often connected to a feedback resistor or ground. The difference between the voltages at these terminals dictates the op-amp's output voltage. $+V$ and $-V$ function as power supply terminals, providing positive and negative voltage sources essential for the op-amp's operation. The range of the op-amp's output voltage depends on the magnitude of these power supply voltages, typically falling within the range of 5V to 15V for most op-amps. V_{out} serves as the output terminal where the amplified or processed signal is delivered. The op-amp's output voltage is proportionate to the difference between the input voltages at $V+$ and $V-$, multiplied by the op-amp's gain, determined by the circuit's configuration and resistor values [41].

Op-amp signal conditioning include gain adjustment, where the ratio of output voltage to input voltage is modified using feedback resistors to match signal levels or amplify weak signals. Offset correction addresses small output voltage variations when the input voltage is zero, minimizing errors in low-level or high-gain applications [36]. Filtering removes unwanted frequencies or noise from the output signal using capacitors, inductors, or resistors in various combinations, such as low-pass, high-pass, band-pass, or notch filters [42].

Linearization ensures the output signal is proportional to the input signal over a wide range, correcting nonlinear responses from sensors or transducers using diodes, transistors, or resistors in different configurations [43]. These signal conditioning techniques contribute to simplifying calibration, measurement, or analysis, as well as improving the accuracy and resolution of the overall system.



CHAPTER 3

METHODOLOGY

3.1 Introduction

This chapter discussed the methods used to advance this research through each step. Methodology refers to the collection of techniques that researchers use to explain, describe, define, and predict phenomena. The next section will give an overview of the work process, followed by a detailed description. This project involves the theoretical and experimental investigation of the growth of ZnO nanorods on glass substrates at three different durations for 3 hours, 6 hours, and 9 hours.

To achieve the aim stated in Chapter 1, the flowchart in Figure 3.1 was adapted to show the research process. The flowchart is important because it shows how the research was conducted in each stage and direction. It details what was done, how it was done, and what steps were followed to reach the research objectives.

Before getting the final results, several stages were completed for this project by constantly referring to the study planning flowchart. One of the processes involved conducting a literature review using journals, articles, or other relevant sources. For this project, it was expected that relevant publications and articles would provide essential information for the design and parameter calculation.

The performance of the coated glass substrates was analyzed through humidity detection, with a specific focus on forward and backward scattering effects. At the conclusion of this project. The LCD display show the voltage reading for each fabricated Zinc Oxide nanorods samples with forward and backward scattering effect.

3.2 Project Flowchart

To satisfy the objectives of the project, a flow chart is refined to illustrate the methodology for the study as shown in Figure 3.1. The project sensor setup were designed for forward and backward scattering measurement using Thinker CAD before the body sensor is constructed using 3D printing technology. The design of the sensor body setup has replaceable glass substrate. An LED and a photodiode were placed 3cm away from the glass substrate, with the photodiode at a 30° angle from the substrate holder. Another photodiode was placed at the edge of one side of the substrate. The LED and the photodiodes acted as the light source and the detectors. Then, ZnO nanorods was fabricated on the glass substrates surface with different growth duration, specifically 3 hours, 6 hours, and 9 hours by using hydrothermal method. The body sensor with forward and backward scattering measurement were then integrated with the fabricated glass substrates samples. This setup was tested in a controlled chamber for analyzing the scattering effect to observe the response of the fabricated sensor specifically on forward and backward scattering towards humidity sensing.

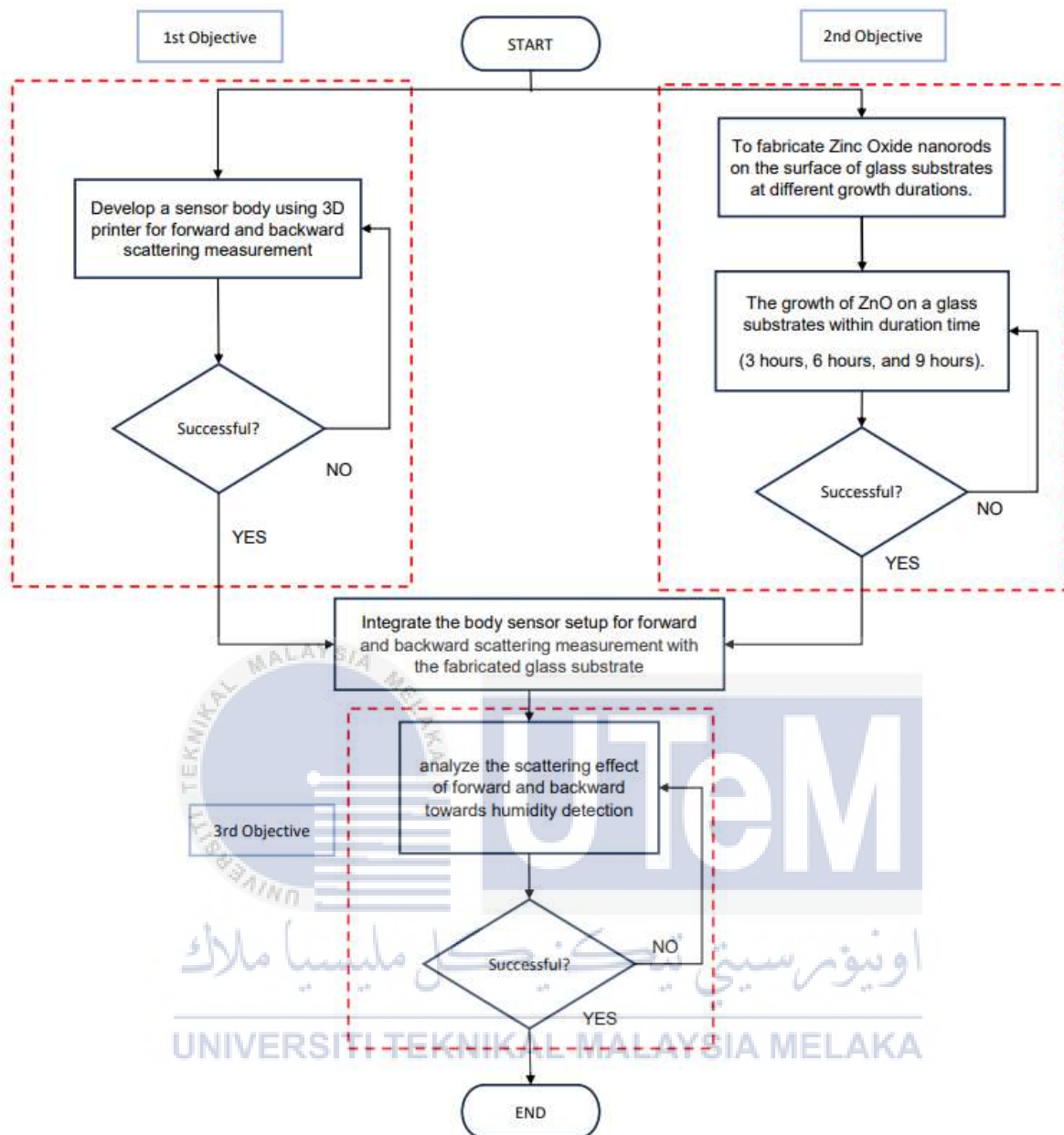


Figure 3.1: Project Flowchart

3.3 Design of Body Sensor Setup

The green LED was utilized to build a low-cost sensor device besides more sensitive to humidity, the wavelength of green light is closer to the absorption wavelength of water molecules than the wavelength of red and blue light. This means that green light is more likely to be scattered by water molecules, resulting in a stronger signal for the sensor to detect. To capture and measure light signals, photodiodes of the SFH203 [28] model were used as photodetectors. The sensor body setup was constructed with Polyactic Acid (PLA) material by using 3D printing technology after the design was developed using TinkerCAD software. All involved components included the LED holder, the photodiodes holder, and the glass substrates coated with zinc oxide, which could be replaced as needed. The sensor device was designed with an LED and one photodiode positioned at the edge of the glass substrate, while another photodiode was placed as close as possible to the zinc oxide coating on the glass substrates. These design and fabrication techniques allowed the sensor to consistently record readings in a low-cost setup.

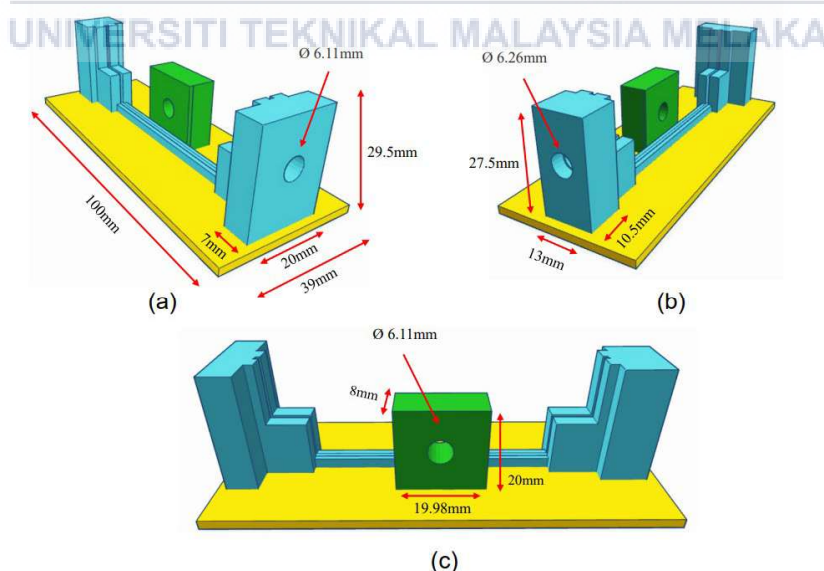


Figure 3.2: Dimension for (a) sensor body setup & Photodiode 1 holder (b) LED holder (c) Photodiode 2 holder

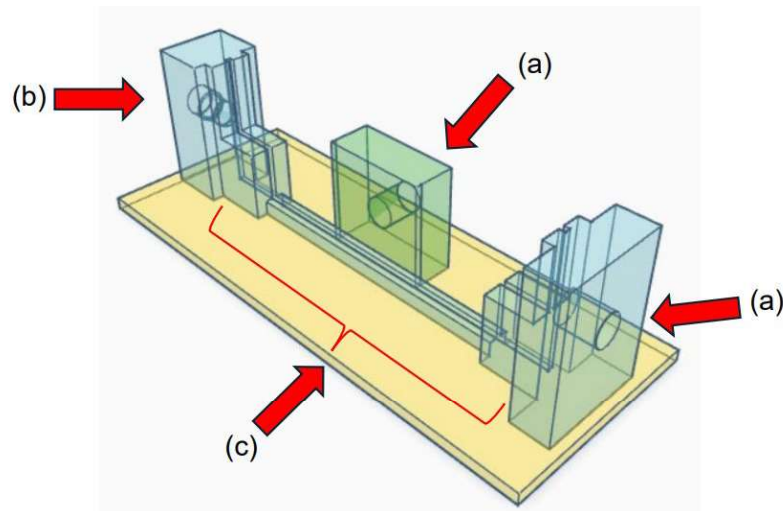


Figure 3.2.1: (a) Photodiode holder (b) LED holder (c) Glass substrate holder

3.4 Circuit Implementation of Receiver

The sensor device captures light passing through both the sample and the region coated with ZnO nanorods. The photodiode at the output converts the collected light into a linearly proportional current. To prevent interference from stray light, a small hole has been designed for backward scattering (sensor 2), while a hole with a diameter of 23.2 mm designed for forward scattering (sensor 1), ensuring minimal light intensity reaches the photodiode. To convert the output current from the photodiode into suitable voltage for processing within the Arduino-based sensing system, a straightforward transimpedance amplifier (TIA) is applied [44]. Figure 3.3 shows the receiver circuit, which integrates the LT1884 [45] op-amp chip. This precision op-amp offers rail-to-rail output swing and picoamp input performance. The input offset voltage is adjusted to be below $50\mu\text{V}$, confirming high precision. Additionally, its low drift conserves accuracy the entire operating temperature range. Moreover, the input bias currents exhibit exceptional performance, with a maximum value of only 400pA . The output voltage of the operational amplifier (op-amp) can be defined as:

$$V_{out} = R_f \times i_d$$

R_f stands for the feedback resistor and i_d is photocurrent. A feedback capacitor (C_f) is contained for stability [45]. The op-amp chip is capable of generating an output voltage of at least 4.7 V. Due to small photocurrent to measure with the standard multimeter, the feedback resistor (R_f) was fine-tuned in the practical system. This adjustment enabled the sensor system to generate a usable output voltage level.

In this project, two circuit design was constructed. The list of components for first circuit design has been listed in Table 3.1 which consists of 5 units of 22 M Ω and 1 unit of 220 Ω resistors, 10 nF capacitor, LT1884 Op-Amp, SFH203 photodiode and bright LED (green color). The second circuit design has been listed in Table 3.1 which consists of resistor 2 M Ω , 10 nF capacitor, LT1884 Op-Amp and SFH203 photodiode. The circuit was designed by using EasyEDA and was constructed as shown in Figure 3.3

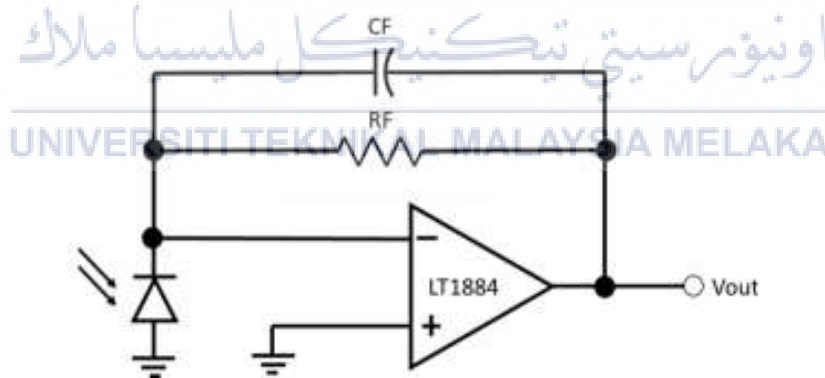


Figure 3.3: A photodiode connected with Transimpedance Amplifier (TIA)


Table 3.1: List of Component.


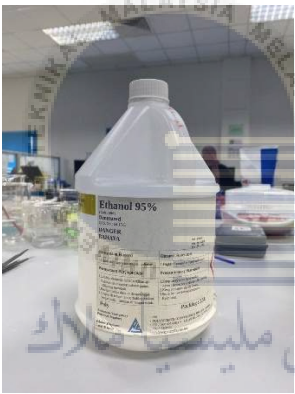

QUANTITY	COMPONENT
5	22 M Ω resistor
1	2 M Ω resistor
2	10 nF capacitor
2	SFH 203 Photodiode
1	Bright LED (Green color)
1	220 Ω
1	LT1884 Op-Amp

3.5 Materials and Equipment

Table 3.2 shows the materials and solution used during the project and Table 3.3 shows the equipment used during the project.

Table 3.2: Material used

NO	MATERIAL	DESCRIPTION
1.	Acetone 	Chemical formula: C ₃ H ₆ O Molar Mass: 58.08 g/mol ⁻¹ Appearance: Colorless liquid with a characteristic pungent and fruity odor

2.	<p>Deionized water (DI Water)</p> 	<p>DI water is crucial in laboratories for solvent preparation, cleaning glassware, and maintaining consistent sample conditions. Its lack of ions ensures accurate experimental results and prevents interference with chemical reactions.</p>
3.	<p>Ethanol</p> 	<p>Chemical formula: C_2H_6O</p> <p>Molar Mass: $46.069 \text{ g/mol}^{-1}$</p> <p>Appearance: Colorless liquid with a characteristics wine-like odor and a pungent taste</p>
4.	<p>Hexamethylenetetramine</p> 	<p>Chemical formula: $C_6H_{12}N_4$</p> <p>Molar Mass: $140.186 \text{ g/mol}^{-1}$</p> <p>Appearance: White crystalline solid</p>


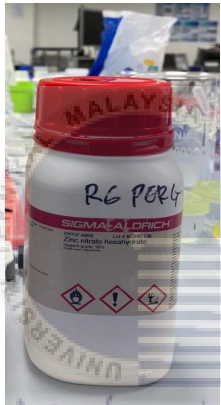









5.	<p>Zinc Acetate Dihydrate</p> 	<p>Chemical formula: $C_4H_{10}O_6Zn$</p> <p>Molar Mass: $219.51 \text{ g/mol}^{-1}$</p> <p>Appearance: White crystalline powder, chunks or chips</p>
6.	<p>Zinc Nitrate Hexahydrate</p> 	<p>Chemical formula: $H_{12}N_2O_{12}Zn$</p> <p>Molar Mass: $297.48 \text{ g/mol}^{-1}$</p> <p>Appearance: Off-white crystalline solid</p>

Table 3.3: Equipment and Device used.

NO	EQUIPMENT	DESCRIPTION
1.	<p>Ender 3D Pro Printer</p> 	<p>Adopts high quality power supply specially designed for 3D printing industry with a stable supply of power.</p>

2.	<p>Filament PLA</p> 	<p>Filament PLA, or Polylactic Acid, is a bioplastic popular in 3D printing due to its unique properties and environmental benefits. PLA offers a more sustainable alternative to traditional plastics. PLA filament is a versatile and eco-friendly choice for a wide range of 3D printing applications, particularly for beginners and projects where sustainability is a priority.</p>
3.	<p>Latex Glove</p> 	<p>Lab safety gloves act as a protective barrier for hands, preventing contamination from harmful substances like chemicals and microorganisms. They create a safe working environment by minimizing the risk of exposure to these hazards. The specific type of gloves used depends on the task and materials being handled in the lab.</p>
4.	<p>Microscope Glass Slide</p> 	<p>It is used as a sensing medium that is fixed into sensor body setup.</p> <p>Thickness: 1 mm</p> <p>Size: 75 mm x 26 mm</p>

5.	<p>PTFE Tape</p> 	<p>It's commonly used for sealing threads and preventing leaks in plumbing and other applications. PTFE tape is used in this project to cover the glass substrate and leave an exposed rectangular area for ZnO nanorod growth.</p>
6.	<p>Pipette Joan Lab</p> 	<p>A tool in chemistry and biology labs, used for sucking up and then carefully dropping a specific amount of liquid. In this project, it's used to add tiny amounts of solution on the glass substrate during an annealing process.</p>
7.	<p>Magnetic Stirrer and Hot Plate</p> 	<p>It is used to mix and heat the solution to create another chemical reactions.</p>

8.	<p>Ultrasonic cleaner</p> 	<p>This equipment uses a special setup with two parts which is an ultrasonicator and a heated water bath. The ultrasonicator uses sound waves to break down molecules in a solution, while the water bath keeps the solution at a steady temperature. In this project, this equipment used for cleaning and a water bath process.</p>
9.	<p>Eco-Cell Laboratory Oven</p> 	<p>Electrically heated ovens/incubators is adjustable-temperature hot air. By using hot air circulation, it can uniformly heat various materials to a precisely controlled temperature.</p> <p>Maximum Temperature: 250°C</p>

3.6 Preparation of Glass Substrates

Figure 3.4 shows the procedures for setting up the glass substrates before the synthesis process. The preparation steps involved the cleaning, drying and masking processes. Several glass substrates were prepared with the purpose of investigating various ZnO nanorods growth conditions.

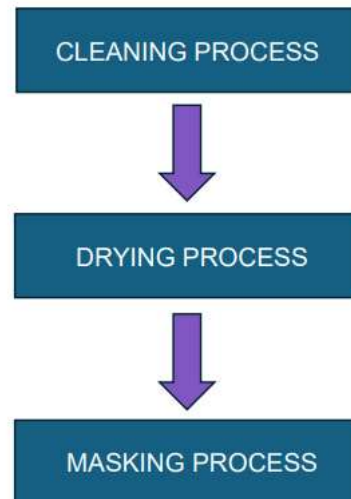


Figure 3.4: Glass substrate preparation process.

In accordance with the procedures shown in Figure 3.4, the glass substrates were initially washed with soap water and then subjected to a 5 min ultrasonic bath using acetone, ethanol, and deionized (DI) water. This cleaning regimen was designed to remove any residues, dirt, or particles from the surfaces of the substrates. Subsequently, the substrates were dried in an atmospheric oven at 70°C for half an hour to ensure they were devoid of any contaminants prior to further processing.

Once dried, the substrates were allowed to return to room temperature. The glass substrates were then masked with polytetrafluoroethylene (PTFE) tape, which left a rectangular area exposed for ZnO nanorod application as shown in Figure 3.5. PTFE was selected for its ability to adhere to glass without additional adhesives, which could potentially interfere with nanorod growth due to chemical reactions.

This research aimed to investigate the impact of ZnO nanorods coated on glass substrates with a rectangular shape on light intensity across different durations. The dimensions of the exposed rectangular section on each substrate were 25mm in length and 20mm in width, as illustrated in Figure 3.5. This setup facilitated the subsequent seeding process for ZnO

nanorods, ensuring a specific area was covered by PTFE tape while leaving the necessary section uncovered.

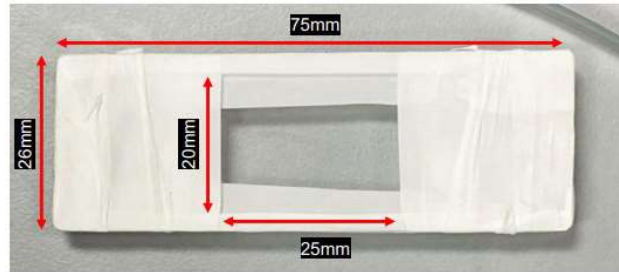


Figure 3.5: Measurement of glass substrates.

3.7 Preparation of Hydrothermal Process

In this project, the growth of ZnO nanorods coated glass substrates was achieved via hydrothermal method. This method involves three main steps which are seeding process, annealing process and growth process that shown in Figure 3.6.



Figure 3.6: Flow of the Hydrothermal Process.

3.7.1 Seeding Process

Figure 3.4 outlines the preparation of the glass substrate, which is masked to achieve specific exposed lengths and diameters for ZnO nanorod growth. The seeding process, crucial for nanorod development, can influence the length, uniformity, density, and diameter of the ZnO nanorods depending on its duration. This process encompasses three main steps: preparation of the seeding solution, creation of nucleation sites on the glass substrate, and annealing. The block diagram of the seeding process is depicted in Figure 3.7.

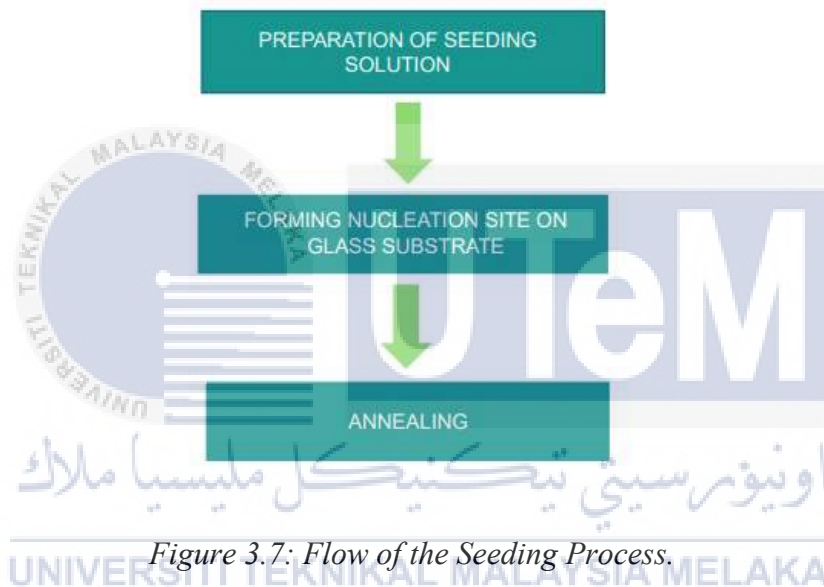


Figure 3.7: Flow of the Seeding Process.

The initial phase of the process involved preparing the seeding solution, as shown in Figure 3.8. A 1 mM concentration of the solution was achieved by dissolving 2.1949 mg of zinc acetate in 10 ml of ethanol. This mixture was then subjected to sonication for several minutes to ensure that the zinc acetate was completely dissolved into the solution.

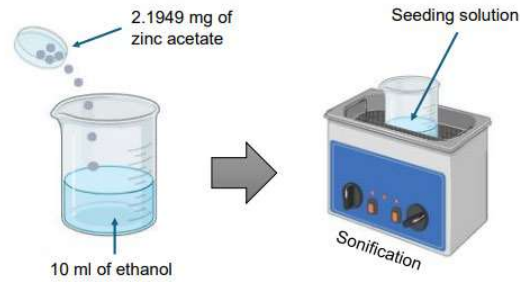


Figure 3.8: Preparation of seeding solution

Figure 3.9 illustrates the seeding process where the masked samples were positioned on a hot plate set to a constant temperature of 70°C to utilize the drop and dry technique, enhancing uniformity. An $80\ \mu\text{l}$ volume of zinc acetate solution was meticulously dispensed onto the exposed areas of each glass substrate using a pipette. Subsequently, the substrates were dried in an oven. This drop casting and drying sequence was performed ten times to ensure adequate coverage and uniformity of the seeding layer. The process of seeding was shown in Figure 3.10.

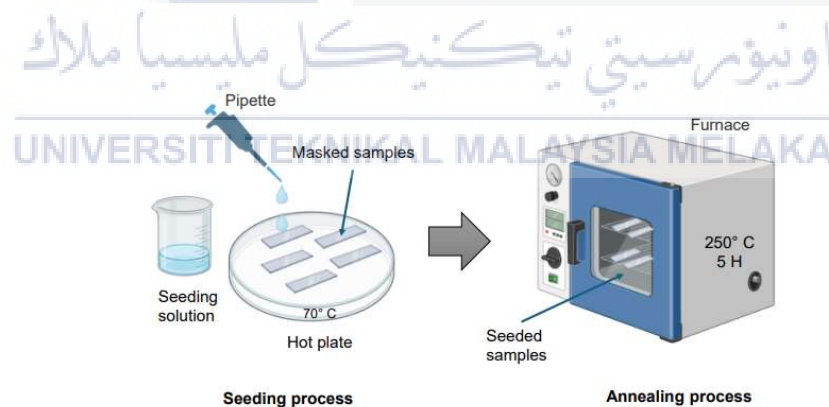


Figure 3.9: Masked samples seeding procedure.

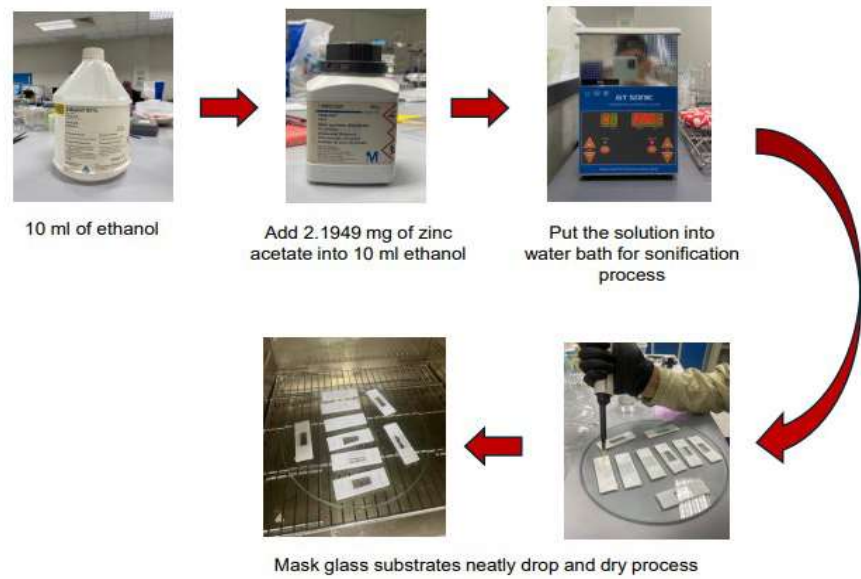


Figure 3.10: Process of Seeding

As illustrated in Figure 3.11, following the seeding stage, the samples underwent an annealing process within an atmospheric furnace. The furnace's temperature increased to 250°C for the annealing phase, which lasted for 5 h. Upon completion, the glass substrates were allowed to cool to room temperature inside the furnace before being removed. This step was essential before moving on to the hydrothermal growth of ZnO nanorods.

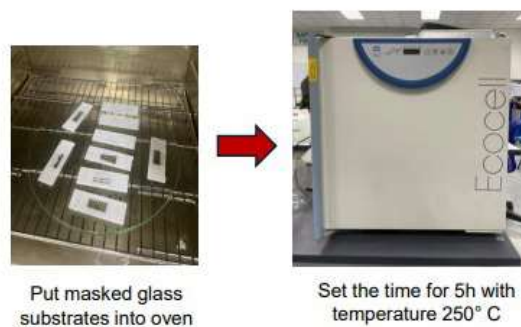


Figure 3.11: Process of Annealing

3.7.2 Growth Process

Figure 3.12 presents the final stage of the hydrothermal coating process, which involves a growth procedure. To create a 10mM solution, 1.18996 g of zinc nitrate hexahydrate ($\text{Zn}(\text{NO}_3)_2 \cdot 6\text{H}_2\text{O}$) and hexamethylenetetramine (HMT) ($\text{C}_6\text{H}_{12}\text{N}_4$) were dissolved in 400 ml of deionized water. A specialized platform was constructed to hold the samples during the growth phase, ensuring an even distribution of the solution over the glass substrates. The masked glass substrates were then heated at 90°C for varying durations 3 h, 6 h, and 9 h in an oven. During this heating process, the substrates were positioned vertically and faced downward into the synthesis solution.

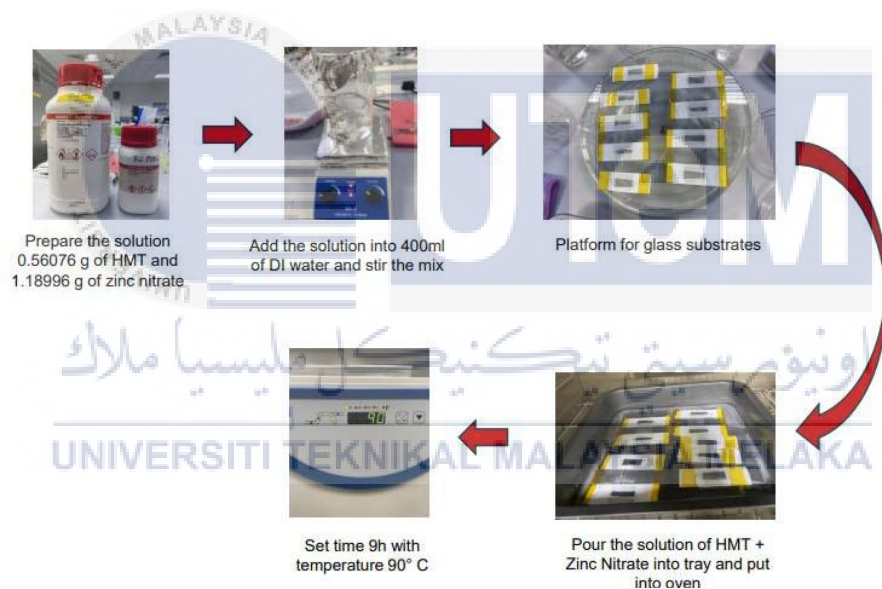


Figure 3.12: Process of Growth

3.8 Humidity Sensing Experiment

Figure 3.13 illustrates the setup used for humidity measurements, featuring a humidity chamber with dimensions of 33 cm (L) x 42.5 cm (W) x 15 cm (H). This chamber was consistently used throughout all experiments. Within this chamber, the sensor device

specifically designed for this research was placed and connected to an Arduino platform to systematically gather data. A hygrometer was also used to verify the actual relative humidity levels.

During the preparation phase, nine samples of ZnO-coated glass substrates were produced, with three samples for each of the growth time durations 3 h, 6 h and 9 h. These samples were processed simultaneously in the same tray.

The experimental procedure involved using silica gel to lower humidity levels and moist tissues to raise them. Humidity was monitored at 5% intervals to ensure stability in both the reduction and increase of humidity levels. Voltage readings were taken at the same time to monitor changes in humidity during the tests.

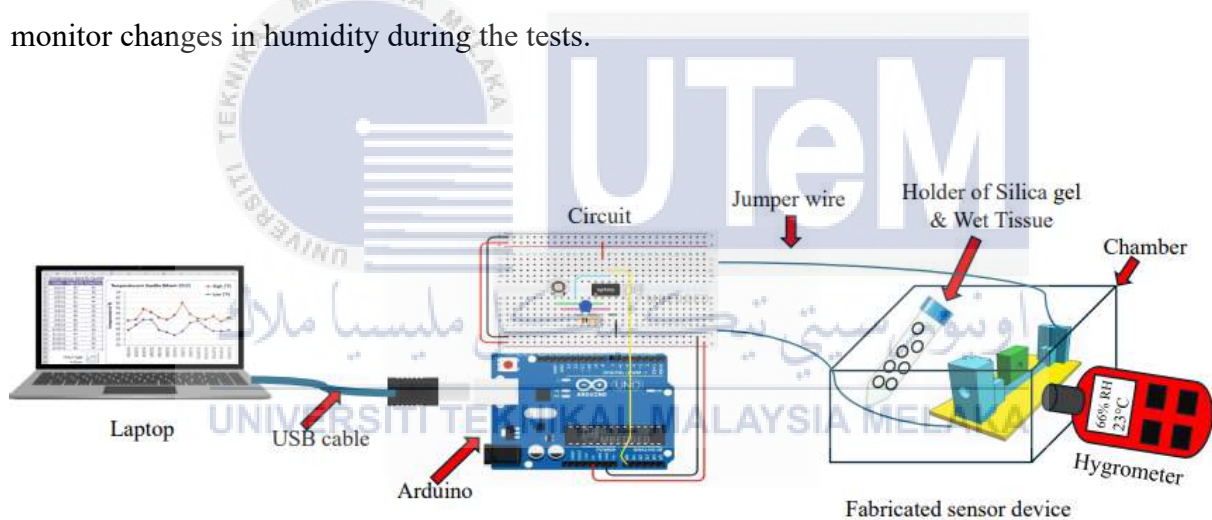


Figure 3.13: Schematic representation of the experimental setup for humidity sensor.

3.9 Stability and Repeatability measurement

In this measurement, the stability of the sensor was thoroughly tested in a controlled chamber where humidity levels were varied from room humidity up to 90%. Initially, the sensor was subjected to room humidity for 10 min, during which the voltage level remained consistently stable. Then, the humidity was increased to 90% and maintained for another 10

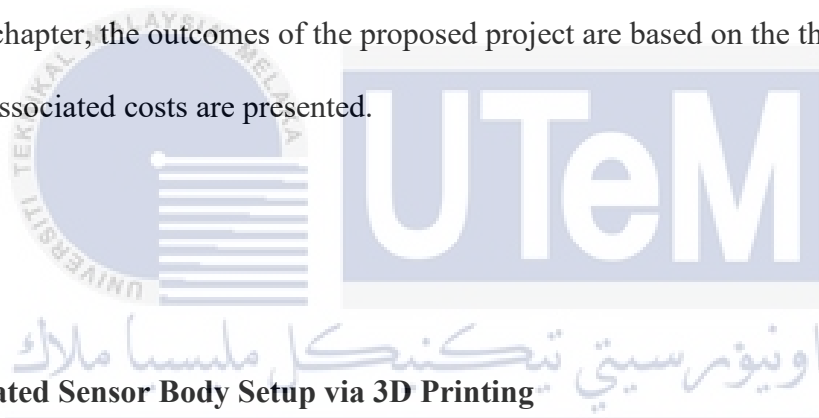
min. The voltage level again remained consistent throughout this period. The sensor's output voltage consistently decreased for forward scattering and increased for backward scattering, returning to normal each time the chamber's humidity was adjusted. This cycle of exposure to different humidity levels was repeated six times to ensure reliability. The entire testing process, lasting about two hours, confirmed the sensor's consistent and reliable performance under changing humidity conditions.



CHAPTER 4

RESULTS AND DISCUSSION

In this chapter, the outcomes of the proposed project are based on the three objectives, as well as the associated costs are presented.



4.1 Fabricated Sensor Body Setup via 3D Printing

Figure 4.1 illustrates the fabrication of the sensor body using an Ender 3D printer. This approach offers several advantages. Firstly, the use of black PLA filament allows for precise printing while minimizing stray light reflection within the sensor system. Stray light can potentially interfere with the sensor's functionality by reaching the photodetectors. Black PLA effectively absorbs this unwanted light, ensuring accurate light detection and measurement. Secondly, 3D printing enables the creation of a customized sensor body design that perfectly fits the overall system requirements. As shown in Figure 4.1, the final sensor body measures 100 mm (length) x 39 mm (width) x 29.5 mm (height), with precisely designed holders for the LED (diameter 6.26 mm) and photodiodes (diameter 6.11 mm). This level of customization ensures optimal light path management and efficient sensor operation.

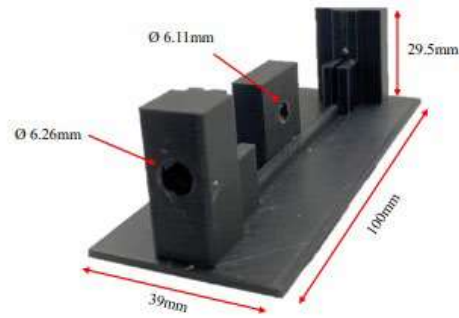


Figure 4.1: The 3D body sensor setup

4.2 ZnO Nanorods on Glass substrates

Figure 4.2 presents an image of the successfully grown ZnO nanorods on glass substrates. These nanorods exhibit a rectangular shape, confirming successful fabrication. As evident from the figure, ZnO nanorod coatings were formed on glass substrates for varying growth durations of 3 h, 6 h, and 9 h. The analysis revealed that after a 9 h growth period, the density of ZnO nanorods within the coating layer was the highest compared to 3 h and 6 h. This translates to a visibly brighter white coating layer on the glass substrate after 9 h of growth. Conversely, the sample exposed to the coating process for only 3 h displayed a slightly clearer layer compared to the others.

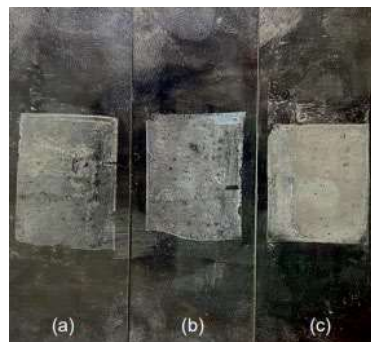


Figure 4.2: ZnO nanorods coating in rectangular shapes on glass substrates for growth duration (a) 3 h (b) 6 h and 9 h.

4.3 Humidity Sensing Setup Integrate with receiver circuit to Arduino Board

Figure 4.3 illustrates an experimental setup for humidity measurement using a sensor device, providing an orthogonal overview. The setup includes three primary components: the connection of a receiver circuit to an Arduino controller board, a chamber that houses the sensor arrangement along with holders for wet tissue and silica gel for humidity control, and a hygrometer to measure ambient humidity levels. The sensor device, designed for this experiment, is placed within the chamber and connected to the Arduino platform, which is in turn connected to a computer or another power source for data logging. A hygrometer, used as a reference for the actual relative humidity levels inside the chamber, is installed outside the chamber wall during the experiment. The electronic components on the receiver circuit's breadboard are powered by the Arduino platform. The LED is powered through the 5 V pin and ground, with a 220 Ω resistor in series. The digital pin is set to a HIGH state, outputting +5 V when activated and returning to 0 V when off. The amplifier on the receiver circuit receives power from the +5 V supply and ground of the Arduino, connected to its V+ and V- inputs. The output signal from the amplifier is sent to the analog pin A0 on the Arduino for analog value reading. This voltage is processed and converted into digital output by the built-in analog-to-digital converter (ADC) of the Arduino, enabling data to be read by a computer.



(a)



(b)

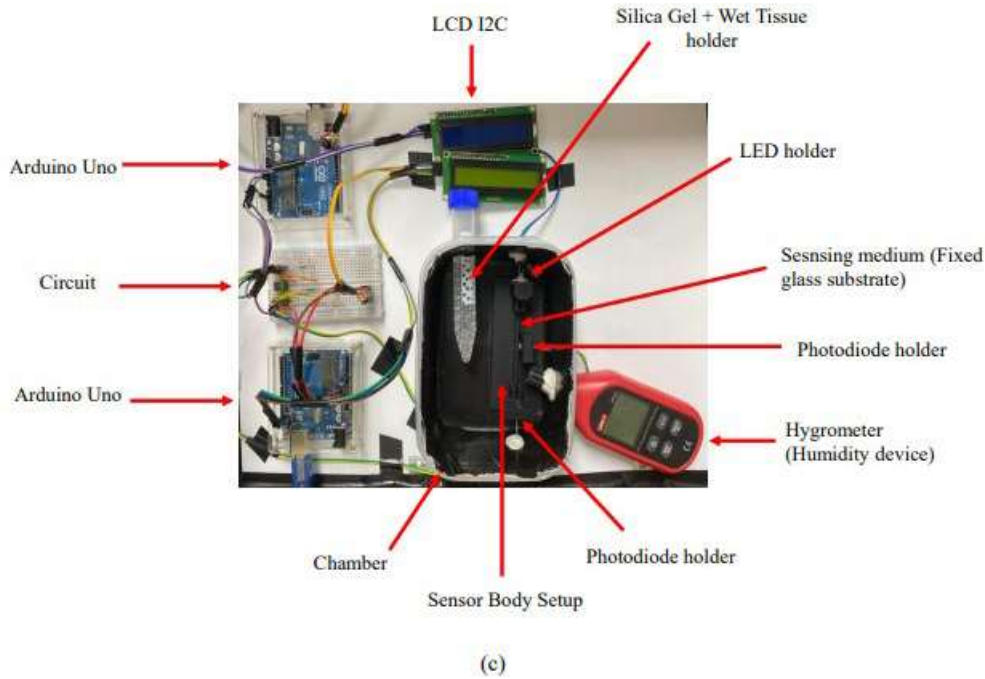


Figure 4.3: Orthogonal overview for the (a) angle view, (b) top view, and (c) full sensor body setup for actual of humidity experiment conducted with integrated sensor device.

4.4 Linearity of intensity

The study considers the principles behind light absorption, as described by Beer-Lambert Law. This law explains how the intensity of light reaching a detector changes based on the amount of material the light travels through can be expressed as [46]

$$I = I_0 e^{-ax} \quad (2)$$

where I_0 is the intensity of light entering the medium, I is the intensity of light leaving the medium, x is the length of the medium, and a is the scattering coefficient. In this method, ZnO nanorod dispersion serves the following purpose is a . Before the light beam reaches the medium's end, it travels through the glass substrate in the direction of the location where the glass substrates with ZnO nanorods were applied. It interacts with the glass substrate-ZnO interface in several places. Because ZnO nanorods have a higher refractive index than air ($n_{\text{air}} \approx 1$), light leakage via them was found under ambient conditions ($n_{\text{zno}} \approx 2$) [47]. The exposure to

high humidity levels significantly impacts the light scattering properties of ZnO nanorods. This phenomenon can be explained by the Beer-Lambert Law, which describes the relationship between light intensity and material properties. The key parameter in this law is the scattering coefficient a , which influences the effective optical properties of the medium. In the case of this sensor, increasing humidity levels cause changes in the value of a for the ZnO nanorods. This alteration is attributed to the interaction of water molecules with the surface of the nanorods, modifying their refractive index (RI). As a consequence, there is a rise in scattering losses within the ZnO layer. In simpler terms, more light gets scattered in various directions rather than traveling directly through the nanorods (forward scattering). This translates to a decrease in the overall light intensity reaching the photodetector. Consequently, the sensor's output voltage exhibits a decline with increasing humidity levels. This response allows the sensor to function as a humidity measurement device by monitoring the changes in voltage.

4.5 Humidity Response

In this experiment, all the growth time samples were test. Each growth duration contains 3 samples which is 3 samples for 3 h, 3 samples for 6 h and 3 samples for 9 h. Sample 1 (S1), sample 2 (S2) and sample 3 (S3) were test with various humidity level. The humidity was measured from 30% to 90% RH levels, the output voltage (V) of the sensor system read by the Arduino platform at every 5% value indicates the amount light the sensor device transmitted.

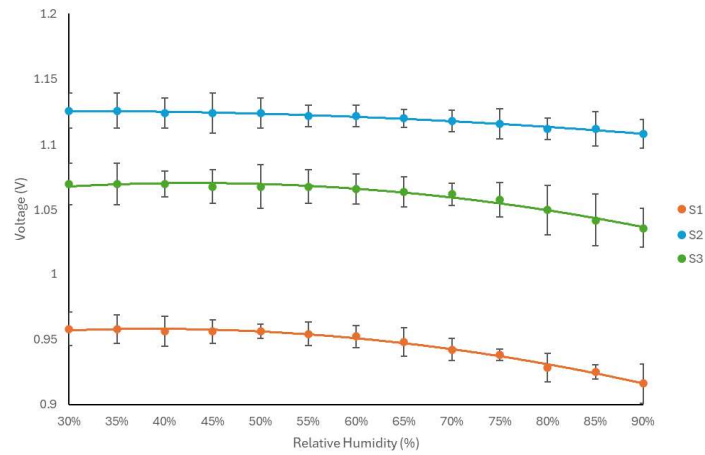


Figure 4.4: Forward Scattering Optical Characterization Towards Humidity Response with 3 h Growth Time samples

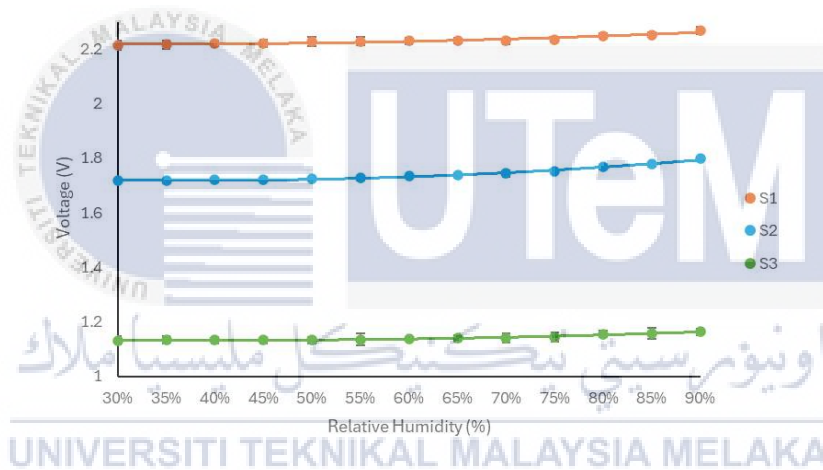


Figure 4.5: Backward Scattering Optical Characterization Towards Humidity Response with 3 h Growth Time samples

Table 4.1: Both Forward and Backward Scattering Optical Characterization Towards Humidity Response with 3 h Growth Time samples

No. of Sample	Forward Average Voltage (ΔV)	Backward Average Voltage (ΔV)
Sample 1	0.07	0.09
Sample 2	0.05	0.10
Sample 3	0.07	0.07

Figure 4.4 and Figure 4.5 show the humidity response for forward and backward scattering respectively for all 3 samples with 3 h growth time. It was observed that the voltage reduced for forward scattering while the voltage increased in backward scattering by nanorods as the humidity increase from 30% to 90%. Table 4.1 summarize the result for 3 h samples and it shows that the sample 1 produced the best sample response among the others.

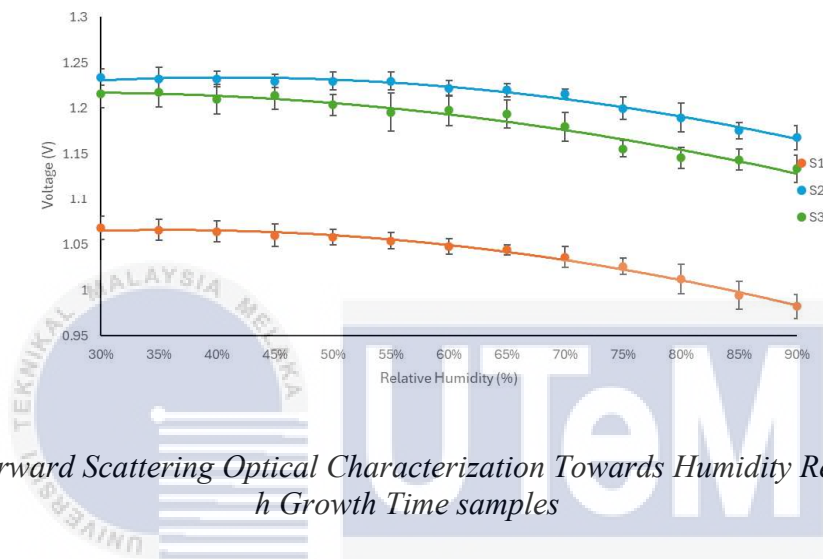


Figure 4.6: Forward Scattering Optical Characterization Towards Humidity Response with 6 h Growth Time samples



Figure 4.7: Backward Scattering Optical Characterization Towards Humidity Response with 6 h Growth Time samples

Table 4.2: Both Forward and Backward Scattering Optical Characterization Towards Humidity Response with 6 h Growth Time samples

No. of Sample	Forward Average Voltage (ΔV)	Backward Average Voltage (ΔV)
Sample 1	0.11	0.13
Sample 2	0.09	0.11
Sample 3	0.11	0.11

Figure 4.6 and Figure 4.7 show the humidity response for forward and backward scattering for all 3 samples with 6 h growth time. Similar to 3 h sample, the result showed identical trend of reduction and increment of voltage for forward and backward scattering, correspondingly. It was also observed that 6 h sample produce much better amount of voltage changes as compared to sample of 3 h. From table 4.2, the amount of voltage changes significantly higher than 3 h samples. From the results, it shows that sample 1 is produce the best response towards humidity among all the sample of 6 h.

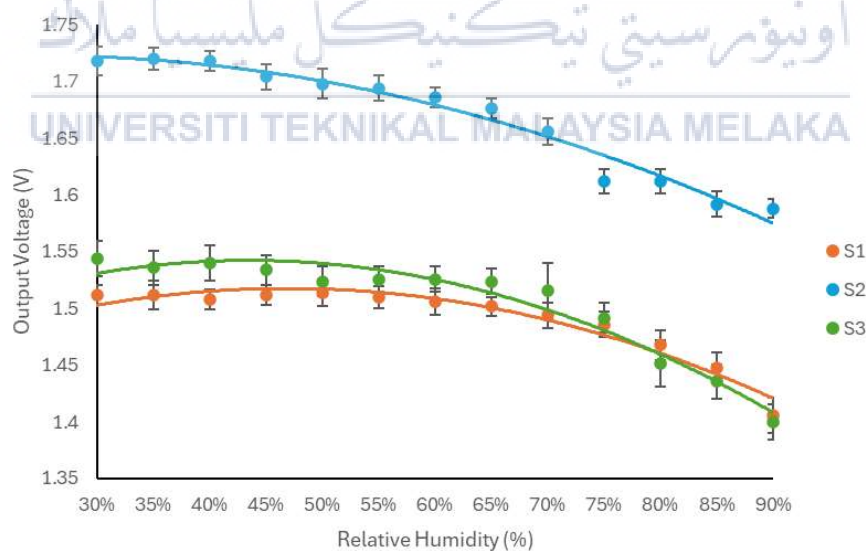


Figure 4.8: Forward Scattering Optical Characterization Towards Humidity Response with 9 h Growth Time samples

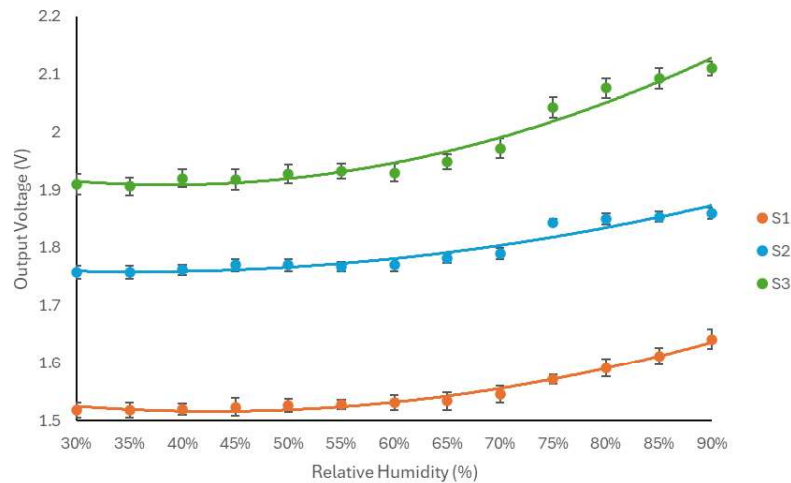


Figure 4.9: Backward Scattering Optical Characterization Towards Humidity Response with 9 h Growth Time samples

Table 4.3: Both Forward and Backward Scattering Optical Characterization Towards Humidity Response with 9 h Growth Time samples

No. of Sample	Forward Average Voltage (ΔV)	Backward Average Voltage (ΔV)
Sample 1	0.14	0.15
Sample 2	0.15	0.15
Sample 3	0.18	0.24

The humidity response for forward and backward scattering for 9 h samples are shown in Figure 4.8 and Figure 4.9 respectively. From the observation from Table 4.3, sample 3 stands out as the best among those grown for 9 h samples because it has the highest average voltage at all levels of humidity tested.

4.6 Comparison ZnO Characteristics for Different Growth Time

Figure 4.10 illustrates the relationship between voltage and relative humidity (RH) for ZnO nanorods with growth durations of 3 h, 6 h and 9 h. Each sample shows a decrease in

voltage as the humidity level increases from 30% to 90%. For further analysis, the best samples from each growth duration were chosen. All samples exhibited a reduction in voltage with increasing humidity. Among these, the 9 h sample produced the highest voltage reduction of 180 mV, followed by the 6 h sample with a reduction of 110 mV, and the 3 h sample with the least reduction of 70 mV. The 3h sample showed a voltage decrease from approximately 0.98 V to 0.91 V, with a total reduction of about 70 mV. The 6 h sample exhibited a voltage drop from about 1.11 V to 1.0 V, showing a reduction of about 110 mV. The 9 h sample experienced a voltage reduction from approximately 1.63 V to 1.45 V, resulting in a reduction of about 180 mV. Overall, the 9 h sample demonstrated the highest sensitivity to humidity changes, making it the most effective for humidity detection among the three samples tested.

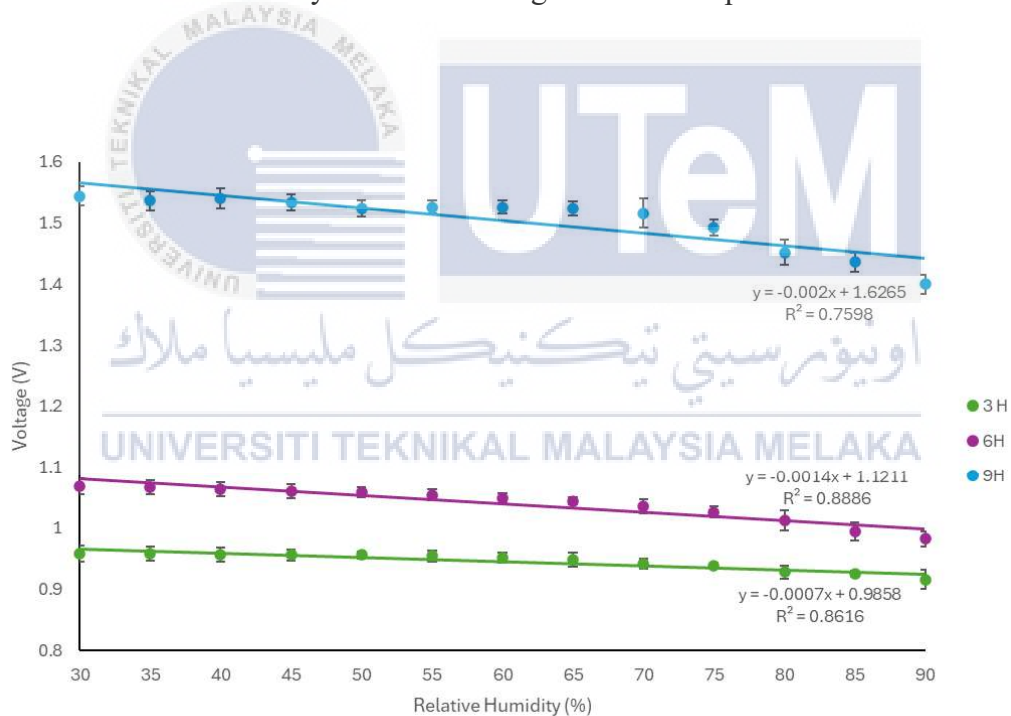


Figure 4.10: Forward Scattering Optical Characterization Towards Humidity Response with different Growth Time

Table 4.4: The output average voltage (ΔV) of forward scattering with different growth time 3 h, 6 h, and 9 h

Growth Time	Forward	Sensitivity	Linearity
(h)	Average Voltage (ΔV)	(mV/%)	
3	0.07	-0.70	0.7598
6	0.11	-1.43	0.8886
9	0.18	-2.40	0.8616

Table 4.4 shows a trend of increased forward scattering with longer growth times. While the average voltage for each growth time increased with humidity (from 0.05 V for 3 h to 0.15 V for 9 h), it's important to note that the voltage increase is relative. This is because the sensor actually receives less light as humidity increases, leading to a decrease in output voltage compared to drier conditions. The observed voltage increase across growth times likely reflects the increasing ability of longer nanorods to scatter light forward, even under higher humidity. It was also observed that 9 h sample produced highest sensitivity of -2.40 mV/% for the forward scattering among all grown samples.

Figure 4.11 shows the comparison between samples 3 h, 6 h and 9 h for backward scattering by nanorods towards humidity detection. Each sample shows an increase in voltage as the humidity level increases from 30% to 90%. Among these, the 9 h sample produced the highest voltage increment during the humidity measurement of 240 mV, followed by the 6 h sample with an increment of 110 mV, and the 3 h sample with the least increment of 90 mV. In contrast, the sensor with a 9 h growth period not only registers the highest initial voltage compared to the 3 h and 6 h durations but also exhibits the most pronounced response to humidity variations.

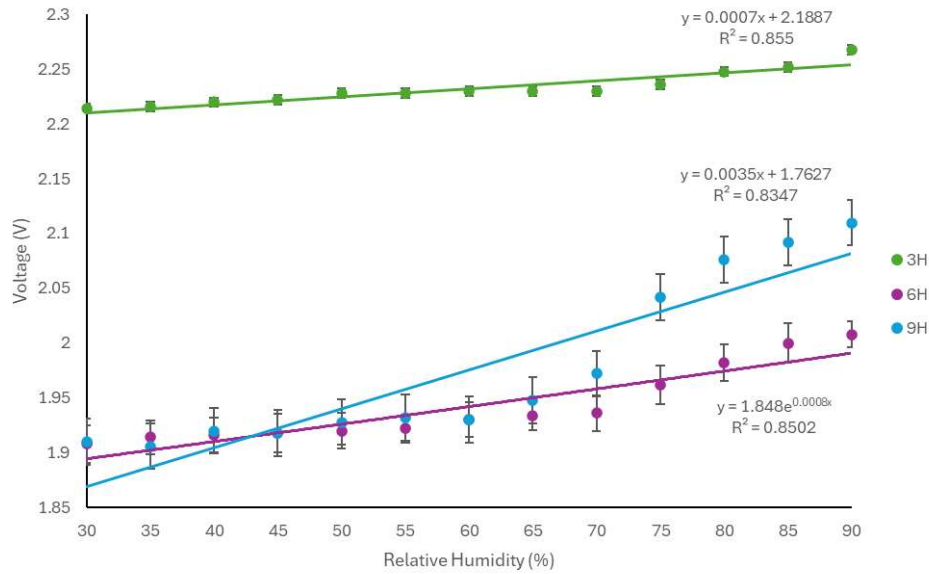


Figure 4.11: Backward Scattering Optical Characterization Towards Humidity Response with different Growth Time

Table 4.5: The output average voltage (ΔV) of backward scattering with different growth time 3 h, 6 h, and 9 h

Growth Time (h)	Backward Average Voltage (ΔV)	Sensitivity (mV/%)	Linearity
3	0.09	0.90	0.8550
6	0.13	1.67	0.8502
9	0.24	3.30	0.8347

Table 4.5 indicates a trend of increased backward scattering with extended growth times. Notably, the average voltage for each growth duration also increased with rising humidity, from 0.09 V for 3 h, 0.13 V for 6 h and 0.24 V for 9 h. This voltage increase is relative, as the sensor detects more light with higher humidity levels. Specifically, elevated humidity causes more light to be reflected back into the glass substrate and towards the sensor

due to decreased light leakage in the forward direction, which complements the increase in backward scattering. Additionally, it was observed that the sample grown for 9 hours exhibited the highest sensitivity for backward scattering, measuring 3.30 mV/% among all the samples tested.

4.7 ZnO Characterization for Different Growth Time

The results presented in Figures 4.10 and 4.11 indicate that the sensor with ZnO nanorods grown for 9 hours exhibits higher sensitivity compared to those grown for 6 and 3 hours. This variation in sensitivity can be attributed to certain unpredictable aspects of the growth process. Variations in material preparation can influence the formation of ZnO, often resulting in increased thickness. Therefore, a prolonged growth 9 h duration leads to thicker ZnO, which correlates with reduced forward light scattering. Table 4.0 and 4.1 corroborates this by showing the decreasing of forward scattering and an increase in backward light scattering.

Previous study [46] has observed that the decreasing of forward scattering light through the nanorods enhances the backward scattering into the glass substrate and towards the photodiode, resulting in increased light detection for the 9 h sample. This happens because the higher adsorption and desorption [47] process of humidity to nanorods, the less light or forward scattering can go through the nanorods. As a result, it was complementing the other scattering which is backward to reflect light through the glass substrate to photodiode. Furthermore, this study acknowledges that optimal light coupling through ZnO growth does not always yield predictable outcomes. This suggests that device performance consistency may not solely depend on modifying ZnO nanorods' morphology, which can introduce variability in device

characteristics. Such disparities can affect the efficacy of these devices in applications like humidity or chemical vapor sensing.

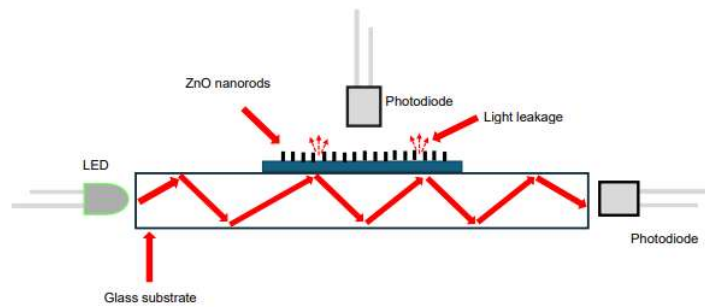


Figure 4.12: Schematic representation of the sensor showing the substrates coated with ZnO nanorods

Therefore, it is proposed that establishing a new standard for sensing device operation is necessary. Theoretically, with extended growth time, backward scattering should intensify. This is empirically supported by all three samples demonstrating increased backward scattering with growth times extending from 3 h to 9 h, confirming that ZnO nanorods enhance their light reflection capabilities over time

Table 4.6: The comparison of output average voltage (ΔV) for forward and backward scattering with different growth time 3 h, 6 h, and 9 h

Growth Time	Forward	Backward
(h)	Average Voltage (ΔV)	Average Voltage (ΔV)
3	0.07	0.09
6	0.11	0.13
9	0.18	0.24

Table 4.6 reveals that samples grown for 9 h exhibit the highest average voltage response for both forward and backward scattering. For forward scattering, the 9 h samples have an average voltage of 0.18 V, compared to 0.11 V for 6 h and 0.07 V for 3 h. Similarly, backward scattering shows the highest response for the 9 h samples (0.24 V) compared to 6 h (0.13 V) and 3 h (0.09 V). Therefore, samples grown for 9 h demonstrate the best overall sensing performance due to their higher average voltage response.

For further analysis Table 4.6 highlights the dominant of backward scattering. For 3 h, the backward scattering voltage difference Δv_B is 0.09 V, which is significantly higher than the forward scattering difference Δv_F of 0.07 V. Similarly, at 6 h, backward scattering dominates with a Δv_B of 0.13 V compared to the forward scattering Δv_F of 0.11 V. Interestingly, for the 9 h sample, it shows the most high gap average voltage from to 3 h and 6 h with sensitive response with Δv_B by 0.24 V and Δv_F by 0.18 V. In conclusion, based on the average voltage response, backward scattering appears to be more dominant after comparing the average voltage response of each growth time.

4.7 Stability Test Analysis

The stability of the sensor was evaluated by placing it in a controlled environment with 66% humidity for 10 minutes. Subsequently, the humidity level within a chamber gradually increased to 90% over 10 minutes and maintained for another 10 minutes. This cycle of increasing humidity, holding it constant, and then decreasing it back to 66% was repeated a total of six times. The entire test took approximately two hours and confirmed the sensor's consistent performance throughout the varying humidity levels.

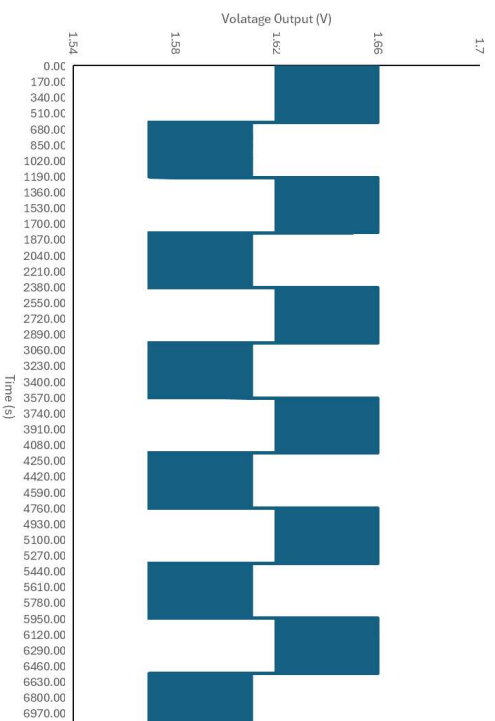


Figure 4.13: The forward sensor stability analysis

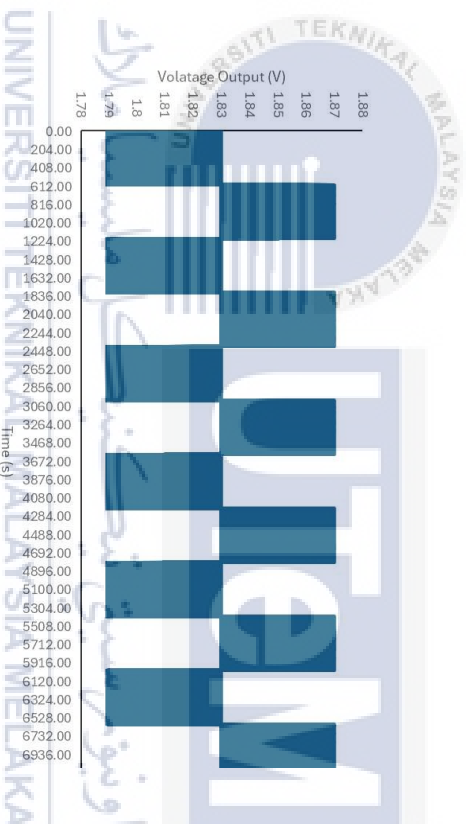


Figure 4.14: The backward sensor stability analysis

Figures 4.13 and 4.14 summarize the repeated testing cycles performed to assess the sensor's stability. The results demonstrate that the sensor maintains stability throughout these cycles. This is shown by the sensor's ability to consistently return to the same voltage level after exposure to high humidity and then back to room humidity. This stability was observed for a total of 6 cycles.

4.8 Environment and Sustainability

This project aligns with Sustainable Development Goal (SDG) 12, which promotes sustainable consumption and production patterns. This project achieves this by presenting a low-cost, integrated humidity sensor device. The device utilizes zinc oxide nanorods, a material fabricated using a simple and environmentally friendly hydrothermal method [48]. Furthermore, the sensor demonstrates promising features for humidity monitoring, including rapid response, high sensitivity, and consistent performance. These characteristics can contribute to preventing issues like corrosion in electronic components, the spread of viruses and bacteria, and the degradation of metal structures through effective humidity control.



CHAPTER 5

CONCLUSION AND FUTURE WORKS

5.1 Conclusion

The 3D printed sensing setup with a built-in receiver circuit capable of measuring forward and backward scattering on ZnO coated glass substrates was successfully achieved with filament PLA by using Ender 3D Pro Printer. The body setup resulted in the glass substrate holder aligned between the LED and one of photodiodes that act as backward scattering and the other one was placed as closed as possible at the tip ZnO nanorods which served as forward scattering. The growth of ZnO nanorods have been successfully coated onto glass substrates via hydrothermal method with a rectangular shape. The fabrication was carried out on three different growth times (3 h, 6 h and 9 h) which resulted in 9 h producing the highest average voltage in both forward and backward scattering. It was observed that longer growth durations decreased light leakage for forward scattering but increased light intensity for backward scattering, as these effects complement each other. This resulted in a higher output voltage. The integrated sensing device was experimentally validated with relative humidity concentrations from 30% to 90%. It was found that the ZnO characteristics towards humidity levels were dominated by backward scattering across all samples of 3 h, 6 h and 6 h of growth times. The maximum reduction of 240 mV was observed

on the backward scattering by sample with growth time of 9 h with sensitivity of 3.3 mV/% for the measurement of relative humidity from 30% to 90%. Furthermore, the sensor device exhibited good stability during the sensor stability test. The output from this analysis shows that sensor is stable for every cycle of the testing where the sensor can move the same voltage level at high humidity and back at the same level to room humidity for 6 cycles. Apart from that, the stability of the body setup during replacement of ZnO samples within the sensor body setup. This study highlights the creation of a sensor that is both affordable and eco-friendly, making it practical for real-world use and environmentally friendly. The findings are useful for other research areas that use ZnO nanomaterials. This analysis provides better understanding and reason on which scattering direction shall researcher focus on in developing a humidity sensing with ZnO nanorods coated onto glass substrates.



5.1 Future Work

Future research should further investigate the capabilities of ZnO nanorods for humidity sensing. The focus could be on analyzing how light is scattered at various angles, which may require the development of a specialized tool for broader angle measurement. Altering the nanorods' physical characteristics, such as shape and size, could also provide valuable insights into their sensitivity to humidity. Precise shaping might be achieved through techniques like electron beam lithography or chemical etching. Additionally, combining light scattering with other detection methods, like measuring electrical signals or vibrations, holds promise for creating more precise and dependable sensors. Testing these sensors in real-life conditions with variable temperatures and air quality is critical. The goal would be to construct a durable sensor prototype and evaluate its performance in these settings. Finally, the ambition is to develop an intricate model that can predict sensor performance based on light scattering

data, potentially utilizing machine learning or detailed analytical methods. Such research endeavors could significantly enhance the design and efficiency of ZnO nanorod-based humidity sensors for various applications.



REFERENCES

- [1] A. Elovitz, Kenneth M, "Understanding what humidity does and why - ProQuest," 1999, Accessed: Nov. 01, 2023. [Online]. Available: <https://www.proquest.com/openview/35d0b3dd65fb5617b63198b19b2731ea/1?pq-origsite=gscholar&cbl=411>
- [2] J. I. Obianyo and J. I. Obianyo, "Humidity Sensors, Major Types and Applications," *Humidity Sensors - Types Appl.*, Jan. 2023, doi: 10.5772/INTECHOPEN.97829.
- [3] C. Bian, J. Wang, X. Bai, M. Hu, and T. Gang, "Optical fiber based on humidity sensor with improved sensitivity for monitoring applications," *Opt. Laser Technol.*, vol. 130, p. 106342, Oct. 2020, doi: 10.1016/J.OPTLASTEC.2020.106342.
- [4] R. Sha, A. Basak, P. C. Maity, and S. Badhulika, "ZnO nano-structured based devices for chemical and optical sensing applications," *Sensors and Actuators Reports*, vol. 4, p. 100098, Nov. 2022, doi: 10.1016/J.SNR.2022.100098.
- [5] S. A. Kamal et al., "A Review of Zinc Oxide (ZnO) Nanostructure Based Humidity Sensor," *Int. J. Nanosci. Nanotechnol*, vol. 19, no. 2, pp. 85–95, 2023, doi: 10.22034/ijnn.2023.1986188.2317
- [6] F. Thakral, G. K. Bhatia, H. S. Tuli, A. K. Sharma, and S. Sood, "Zinc Oxide Nanoparticles: from Biosynthesis, Characterization, and Optimization to Synergistic Antibacterial Potential," *Curr Pharmacol Rep*, vol. 7, no. 1, pp. 15–25, Feb. 2021, doi: 10.1007/S40495-021-00248-7/METRICS.
- [7] M. Javaid, A. Haleem, R. P. Singh, S. Rab, and R. Suman, "Significance of sensors for industry 4.0: Roles, capabilities, and applications," *Sensors International*, vol. 2, p. 100110, Jan. 2021, doi: 10.1016/J.SINTL.2021.100110.

- [8] H. Farahani, R. Wagiran, and M. N. Hamidon, “Humidity Sensors Principle, Mechanism, and Fabrication Technologies: A Comprehensive Review,” *Sensors (Basel)*, vol. 14, no. 5, p. 7881, Apr. 2014, doi: 10.3390/S140507881.
- [9] S. Sikarwar and B. C. Yadav, “Opto-electronic humidity sensor: A review,” *Sens Actuators A Phys*, vol. 233, pp. 54–70, Jul. 2015, doi: 10.1016/J.SNA.2015.05.007.
- [10] “The importance of humidity sensors | Vaisala.” Accessed: Jan. 15, 2024. [Online]. Available: <https://www.vaisala.com/en/expert-article/importance-humidity-sensors>.
- [11] “Humidity Saturation Limits of Hydraulic and Lubrication Fluids.” Accessed: Jan. 15, 2024. [Online]. Available: <https://www.machinerylubrication.com/Read/28697/humidity-saturation-limits>
- [12] C. Pendão and I. Silva, “Optical Fiber Sensors and Sensing Networks: Overview of the Main Principles and Applications,” *Sensors 2022, Vol. 22, Page 7554*, vol. 22, no. 19, p. 7554, Oct. 2022, doi: 10.3390/S22197554.
- [13] “Different Types of Optical Sensors and Applications.” Accessed: Jan. 15, 2024. [Online]. Available: <https://www.elprocus.com/optical-sensors-types-basics-and-applications/>
- [14] “Overview of Photoelectric Sensors | OMRON Industrial Automation.” Accessed: Jan. 15, 2024. [Online]. Available: <https://www.ia.omron.com/support/guide/43/introduction.html>
- [15] N. Sabri, S. A. Aljunid, M. S. Salim, R. B. Ahmad, and R. Kamaruddin, “Toward optical sensors: Review and applications,” *J Phys Conf Ser*, vol. 423, no. 1, 2013, doi: 10.1088/1742-6596/423/1/012064.

- [16] C.-A. ; Ku, C.-K. Chung, C.-A. Ku, and C.-K. Chung, “Advances in Humidity Nanosensors and Their Application: Review,” *Sensors 2023, Vol. 23, Page 2328*, vol. 23, no. 4, p. 2328, Feb. 2023, doi: 10.3390/S23042328.
- [17] T. Linder, “Light Scattering in Fiber-based Materials”.
- [18] N. N. Boustany, S. A. Boppart, and V. Backman, “Microscopic Imaging and Spectroscopy with Scattered Light,” *Annu Rev Biomed Eng*, vol. 12, p. 285, Aug. 2010, doi: 10.1146/ANNUREV-BIOENG-061008-124811.
- [19] R. R. Jones, D. C. Hooper, L. Zhang, D. Wolverson, and V. K. Valev, “Raman Techniques: Fundamentals and Frontiers,” *Nanoscale Research Letters 2019 14:1*, vol. 14, no. 1, pp. 1–34, Jul. 2019, doi: 10.1186/S11671-019-3039-2.
- [20] R. Jayaratne, X. Liu, P. Thai, M. Dunbabin, and L. Morawska, “The influence of humidity on the performance of a low-cost air particle mass sensor and the effect of atmospheric fog,” *Atmos Meas Tech*, vol. 11, no. 8, pp. 4883–4890, Aug. 2018, doi: 10.5194/AMT-11-4883-2018.
- [21] “Relative Humidity - an overview | ScienceDirect Topics.” Accessed: Jan. 15, 2024. [Online]. Available: <https://www.sciencedirect.com/topics/agricultural-and-biological-sciences/relative-humidity>
- [22] J. Huang, B. Wang, and K. Ni, “Improving the Sensitivity of Humidity Sensor Based on Mach-Zehnder Interferometer Coated with a Methylcellulose,” *Int J Opt*, vol. 2018, 2018, doi: 10.1155/2018/5680128.
- [23] A. A. Ensafi, Z. Saberi, and N. Kazemifard, “Functionalized nanomaterial-based medical sensors for point-of-care applications: An overview,” *Functionalized Nanomaterial-Based Electrochemical Sensors: Principles, Fabrication Methods*,

- and Applications*, pp. 277–308, Jan. 2022, doi: 10.1016/B978-0-12-823788-5.00018-1.
- [24] V. Singh Bhati, M. Hojamberdiev, and M. Kumar, “Enhanced sensing performance of ZnO nanostructures-based gas sensors: A review,” *Energy Reports*, vol. 6, pp. 46–62, 2020, doi: 10.1016/j.egy.2019.08.070.
- [25] A. Kolodziejczak-Radzimska and T. Jesionowski, “Zinc Oxide—From Synthesis to Application: A Review,” *Materials*, vol. 7, no. 4, p. 2833, 2014, doi: 10.3390/MA7042833.
- [26] G. Liu, “Hydrothermal synthesis of vanadium dioxide nanoparticles and its applications”, doi: 10.32657/10356/151086.
- [27] L. Ndlwana *et al.*, “Sustainable Hydrothermal and Solvothermal Synthesis of Advanced Carbon Materials in Multidimensional Applications: A Review,” *Materials 2021, Vol. 14, Page 5094*, vol. 14, no. 17, p. 5094, Sep. 2021, doi: 10.3390/MA14175094.
- [28] S. K. K. W. J. H.H.M.Yusof, "Low-Cost Integrated Zinc Oxide Nanorods Based Humidity Sensors for Aduino Platform," *IEEE Sensors Journal*, 2018.
- [29] P. V. K. & J. M. Aneesh, " Synthesis of ZnO nanoparticles by Hydrothermal Method.," *Nanophotonic Materials IV*, vol. 32, pp. 317-320, 2007
- [30] & K. K. Saidin, "Hydrothermal Growth of ZnO: A substratedependent study on nanostructures formation," *IOP Conference Series: Material Science and Engineering*, no. 012016, p. 298, 2018.

- [31] M. Jin, S. Yan, and D. Chen, “Adsorption mechanism of water molecules on the surface of ZnO-SAW sensors,” *Chem. Phys.*, vol. 538, Oct. 2020, doi: 10.1016/J.CHEMPHYS.2020.110915.
- [32] H. Ye, G. Chen, H. Niu, Y. Zhu, L. Shao, and Z. Qiao, “Structures and mechanisms of water adsorption on ZnO(0001) and GaN(0001) surface,” *J. Phys. Chem. C*, vol. 117, no. 31, pp. 15976–15983, Aug. 2013, doi: 10.1021/JP312847R.
- [33] M. Khan, M. M. Rehman, S. A. Khan, M. Saqib, and W. Y. Kim, “Characterization and performance evaluation of fully biocompatible gelatin-based humidity sensor for health and environmental monitoring,” *Front Mater*, vol. 10, p. 1233136, Jul. 2023, doi: 10.3389/FMATS.2023.1233136/BIBTEX.
- [34] “(PDF) Development of NO₂ gas sensor based on Ti modified ZnO nanowires.” Accessed: Jan. 15, 2024. [Online]. Available: https://www.researchgate.net/publication/321746813_Development_of_NO2_gas_sensor_based_on_Ti_modified_ZnO_nanowires
- [35] J. Yan, A. Chen, and S. Liu, “Flexible sensing platform based on polymer materials for health and exercise monitoring,” *Alexandria Engineering Journal*, vol. 86, pp. 405–414, Jan. 2024, doi: 10.1016/J.AEJ.2023.11.085.
- [36] C. Yu *et al.*, “Application of Through Glass Via (TGV) Technology for Sensors Manufacturing and Packaging,” *Sensors 2024, Vol. 24, Page 171*, vol. 24, no. 1, p. 171, Dec. 2023, doi: 10.3390/S24010171.
- [37] “Low-Cost Data Acquisition (DAQ) with Arduino and Binho for ML.” Accessed: Jan. 15, 2024. [Online]. Available: <https://www.digikey.my/en/maker/projects/lowcost-data-acquisition-daq-with-arduino-and-binho-for-ml/bf39a39f07d145d297e60c0e1f257db3>

- [38] “Analog to Digital Conversion - SparkFun Learn.” Accessed: Jan. 15, 2024. [Online]. Available: <https://learn.sparkfun.com/tutorials/analog-to-digital-conversion/all>
- [39] “Arduino Integrated Development Environment (IDE) v1 | Arduino Documentation.” Accessed: Jan. 15, 2024. [Online]. Available: <https://docs.arduino.cc/software/ide-v1/tutorials/arduino-ide-v1-basics>
- [40] “Operational Amplifier Basics - Op-amp tutorial.” Accessed: Jan. 15, 2024. [Online]. Available: https://www.electronics-tutorials.ws/opamp/opamp_1.html
- [41] “Op-Amp Practical Considerations | Operational Amplifiers | Electronics Textbook.” Accessed: Jan. 15, 2024. [Online]. Available: <https://www.allaboutcircuits.com/textbook/semiconductors/chpt-8/op-amp-practical-considerations/>
- [42] “Passive Low Pass Filter - Passive RC Filter Tutorial.” Accessed: Jan. 15, 2024. [Online]. Available: https://www.electronics-tutorials.ws/filter/filter_2.html
- [43] T. Islam and S. C. Mukhopadhyay, “INTERNATIONAL JOURNAL ON SMART SENSING AND INTELLIGENT SYSTEMS 1 Linearization of the sensors characteristics: a review,” vol. 12, 2019, doi: 10.21307/ijssis-2019-007.
- [44] R. Keim, "Design Tips for Photodiode Amplifier," All about circuit, 21 January 2021. [Online]. Available: <https://www.allaboutcircuits.com/technical-articles/design-tips-forphotodiode-amplifiers/>. [Accessed 5 April 2024].
- [45] "LT1884 Datasheet and Product Info," Analog Devices, 23 August 2007. [Online]. Available: <https://www.analog.com/en/products/lt1884.html#product-overview>. [Accessed 5 April 2024].

- [46] S. M. H. F. S. T. S. W. H. W. S. M. Hazli Rafis, "Side coupling of multiple optical channels by spiral patterned Zinc Oxide coatings on large core plastic optical fibers.," *Micro & Nano letters*, vol. 11, no. 2, pp. 122-126, 2016
- [47] H.-K. S. S. H. Y. J. S.-H. H. J.-S. K. S. P. S.-E. & C. J. Kim, "Humidity Sensing Properties of Nanoporous TiO₂-SnO₂ Ceramic Sensors," *Bulletin of the Korean Chemical Society*, vol. 26, no. 11, pp. 1881-1884, 2014.
- [48] "Goal 12: Responsible consumption and production.," *The Global Goals.*, 18 April 2023. [Online]. Available: <https://www.globalgoals.org/goals/12-responsible-consumption-and-production/>. [Accessed 14 June 2024].
- [49] C. Elosua, I. R. Matias, C. Bariain, and F. J. Arregui, "Volatile organic compound optical fiber sensors: A review," *Sensors*, vol. 6, no. 11, pp. 1440–1465, 2006, doi: 10.3390/S6111440.
- [50] U. S. Sainadh, S. N. Sandhya, R. Vathsan, and A. Narayanan, "Weak value amplification in resonance fluorescence," *Curr. Sci.*, vol. 109, no. 11, pp. 2002–2005, 2015, doi: 10.18520/V109/I11/2002-2005.
- [51] "(PDF) Design and Development of a Coherent Detection Rayleigh Doppler Lidar System for Use as an Alternative Velocimetry Technique in Wind Tunnels." https://www.researchgate.net/publication/343770420_Design_and_Development_of_a_Coherent_Detection_Rayleigh_Doppler_Lidar_System_for_Use_as_an_Alternative_Velocimetry_Technique_in_Wind_Tunnels (accessed Jan. 20, 2024).
- [52] Bruker, "Guide to Raman Spectroscopy | Bruker," 2023. <https://www.bruker.com/en/products-and-solutions/infrared-and-raman/raman-spectrometers/what-is-raman-spectroscopy.html> (accessed Jan. 20, 2024).

- [53] “(PDF) A Semi-Analytic Model of Fog Effects on Vision.”
https://www.researchgate.net/publication/281695717_A_SemiAnalytic_Model_of_Fog_Effects_on_Vision (accessed Jan. 20, 2024).
- [54] Z. Liu, Q. Cai, C. Ma, J. Zhang, and J. Liu, “Photoelectrochemical properties and growth mechanism of varied ZnO nanostructures,” *New J. Chem.*, vol. 41, no. 16, pp. 7947–7952, 2017, doi: 10.1039/C7NJ01725A.

